Contents

1. Vascular development and dioxin toxicity

Dioxin and related compounds, which belong to a family of halogenated aryl hydrocarbons, are produced unintentionally in uncontrolled combustion processes and in various types of industrial processes [1]. Among more than 400 kinds of congeners depending on the number and position of chlorine atoms on the benzene ring, 2,3,7,8-tetrachlorodibenzo-*p*-dioxin (TCDD) has been established as the most toxic congener on the basis of experimental studies. The fetus is one of the most sensitive targets in the life of mammals, and *in utero* and lactational exposure to dioxins has been reported to elicit a wide spectrum of biological and toxicological responses, including reproductive, neurobehavioral, and immune disturbances in the offspring, by which dams are not affected as much as their fetuses [2]. Among the wide spectrum of toxicities, vascular development is particularly sensitive to the toxic effects of TCDD compared with congenital malformations or birth defects. Previous studies demonstrated that exposure to TCDD during development results in heart size reduction in the piscine embryo [3,4], dilatation of ventricular cavity associated with thinner ventricle walls in the chicken embryo [5] and decrease in heart-to-body weight in mice [6], all of which were accompanied by the reduction in cardiomyocyte proliferation. Edema and hemorrhage were observed and considered as common features of TCDD toxicities in the vasculature irrespective of animal species. Exposure to TCDD *in utero* induced subcutaneous edema and intestinal hemorrhages in the fetuses of the rat and hamster [7], and resulted in leakage from the vasculature in the morbid avian and piscine embryos, the latter of which was confirmed by severe subcutaneous, pericardial, and peritoneal edema prior to death [5,8]. TCDD clearly has a strong impact on living organisms by causing damage to the vascular system.

The toxicity of TCDD is mediated by the binding of TCDD to the arylhydrocarbon receptor (AhR), which is then activated. The activated ligand-bound AhR translocates to the nucleus from the cytoplasm and dimerizes with the aryl hydrocarbon receptor nuclear translocator (ARNT), followed by the binding of this AhR/ARNT heterodimer to the xenobiotic response element (XRE; also known as the dioxin response element, DRE) in the promoter region of a various genes [9]. If the XRE elements are functional, the AhR/ARNT heterodimer modulates the expression of those genes, including drug-metabolizing enzymes, i.e., phase I enzymes such as CYP1A1 and 1B1 and phase II enzymes such as UDP-glucuronosyl transferase, and biological and toxicological responses will emerge.

The vascular network plays a critical role at the very beginning of embryo development in order to supply oxygen and nutrients to adjacent proliferating or differentiated cells. Vasculature development in most of the organs is relatively simple and depends on two consecutive processes, vasculogenesis and angiogenesis [10] (Fig. 1A). In vasculogenesis, blood vessels form through the *in situ* differentiation between undifferentiated precursor cells, called angioblasts, to endothelial cells that assemble into a primitive vascular network, in which the adhesion of endothelial cells and periendothelial support cells is at the immature stage. The term angiogenesis was used to generally denote the growth and remodeling of the primitive network into a complex network. During this remodeling, periendothelial support cells are recruited to encase endothelial tubes, resulting in the maturation of blood vessels. In addition, some preexisting vessels send out capillary sprouts to produce new vessels. At each of these stages, growth factors and their receptors have been identified to act as modulators [10]. The vascular endothelial growth factor (VEGF) and its receptors (VEGFRs), such as fetal liver kinase-1 (Flk1) and fms-like tyrosine kinase-1 (Flt1), named the VEGF/VEGFR system, are mainly associated with vasculogenesis. Angiopoietin-1 (Ang1) and Ang2 and their receptor Tie2, named the Ang/Tie2 system, are involved mainly in angiogenesis, or vascular remodeling. Vascular development is basically stimulated under a hypoxic condition, which is dependent on transcription factors known as the hypoxia-inducible factors (HIFs). Under normal oxygen tension, HIF-1α is posttranslationally modified and subsequently degraded through the proteasome. However, under hypoxic conditions, HIF-1α can escape from degradation, and the accumulated HIF-1α binds to the oxygen-insensitive molecule known as the ARNT, also called HIF-1β. The HIF-1α/ARNT heterodimer subsequently binds to the hypoxia response element (HRE) in the promoter region of genes involved in the adaptation to hypoxia. Thus, the HIF-1α acts as a master regulator to activate the transcription of many hypoxia-response genes, including the VEGF/VEGFR or Ang/Tie2 system, and regulates the expressions of VEGF, Flt1, and Ang2 [11].

HIF-1α plays its intrinsic role in hypoxia signaling, and presumably modulates dioxin toxicities because of its ability to heterodimerize with ARNT [11]. In other words, ARNT is a common transcription factor that shares its role with AhR and HIF-1α to modulate XRE- and HRE-dependent pathways, respectively. Thus, it has been speculated that the AhR/ARNT and HIF-1α/ARNT pathways affect each other by competing for the limited quantities of ARNT molecules [12] (Fig. 1B).

Although it is considered that ARNT does not act as a limiting factor for the interaction with either AhR or HIF-1α because ARNT is abundant in cells under basal physiological condition [13], some of the experimental observations might be explained by the former hypothesis. In a study by Ichihara et al. [14], hypoxia caused by the ligation of the femoral artery was found to induce angiogenesis more significantly in AhR-null mice than in wild-type mice. In this study, electrophoretic mobility shift assay (EMSA) analysis showed that the DNA binding activity of the HIF-1α and ARNT complex is more pronounced in the AhR-null mice than in the wild-type mice under ischemic conditions. Thus, the authors suggest that the increased quantity and activity of the HIF-1α/ARNT heterodimer in ischemia-induced AhR-null mice may explain at least in part the enhancement of ischemia-induced VEGF expression and angiogenesis. In a study by Fritz et al. [15], transgenic adenocarcinoma of the mouse prostate (TRAMP) mice having AhR-null mutation develop prostate tumors with greater frequency than AhR-positive TRAMP mice. The authors showed that the stimulated development of the prostate tumor in AhR-null TRAMP mice is due to the accelerated angiogenesis resulting from the increased VEGF expression on the prostate epithelial hyperplasia, a typical malformation observed in TRAMP mice. Because the addition of vanadate, a putative inducer of the HIF-1α-VEGF pathway, resulted in VEGF induction in the organ culture experiment of the prostate obtained from AhR-null mice but not from WT mice, the authors concluded that the increased VEGF production in AhR-null TRAMP mice is due to the overstimulated HIF-1α/ARNT signaling pathway. On the other hand, exposure to TCDD or 3-methylcholanthrene decreased the VEGF expression under several experimental conditions such as in the case of coronary endothelial tube formation in chick embryos [16–18] and human umbilical vein endothelial cells (HUVECs) *in vitro* [19]. Exposure to cigarette smoke extract was shown to suppress the hypoxia-induced cellular migration and capillary-like tubule formation in HUVECs *in vitro*. In an *in vivo* experiment, blood flow perfusion in surgically induced ischemic hind limbs was significantly reduced in mice exposed to cigarette smoke. In these *in vitro* and *in vivo* experiments, the expression of HIF-1α/VEGF was downregulated [20]. These observations suggest that the AhR-dependent reduction of VEGF expression by TCDD and other AhR ligands may result in a tilted balance toward the AhR/ARNT pathway instead of the HIF-1α/ARNT pathway. It should be noted that the term 'angiogenesis' has often been used to include the

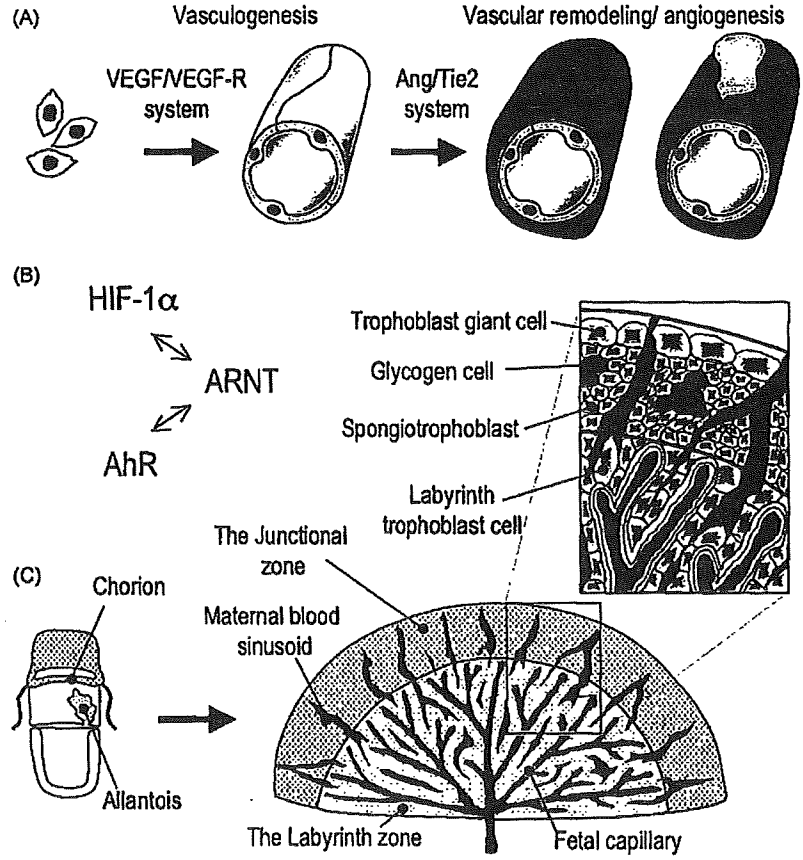

Fig. 1 – Vascular development and structure in the peripheral blood vessels and placenta. (A) In the peripheral blood vessels, a primitive vascular tube is formed during vasculogenesis, which is further processed by remodeling its structure to recruit peripheral endothelial support cells and by sending out capillary sprouts to produce new vessels. (B) Proposed model for suppressive effects of AhR-mediated signaling on HIF-1α signaling pathway by competing for limited amounts of ARNT. (C) Development of the rodent placenta. Placental development is initiated by fusing two membranes, the chorion and allantois. The mature rodent placenta is composed of the labyrinth and junctional zones as described in the text.

term 'vasculogenesis' in a number of papers, and thus, one has to pay particular attention to the blood vessel development stage described in a given paper. Generally, it is plausible to think that not only the vascular remodeling but also vasculogenesis is considered to be a target of AhR ligands.

Although it is still controversial, competition of AhR and HIF-1α with ARNT is a plausible model to work on to elucidate the inhibitory mechanisms of the AhR-mediated signaling pathway on HIF-1α signaling activity. Intriguingly, Ohtake et al. recently found a novel function of AhR [21,22]. The AhR has E3 ubiquitin-ligase activity by forming multiple protein complexes and degraded several transcription factors including the estrogen and androgen receptors. The substrates for AhR-mediated ubiquitin ligase have not been fully identified, and thus, whether HIF-1α is a target of AhR-mediated ubiquitin-ligase activity is yet unknown. In either case, the inhibitory effect of the AhR-mediated signaling pathway on the HIF-1α signaling pathway is due to the downregulation of active HIF-1α, which is consistent with the results of *in vivo* studies. Another possibility of the inhibitory effect of HIF-1α on AhR-mediated gene transcription is a competition of transcription cofactors between these nuclear receptors. Several nuclear receptor coactivators are known to interact with the AhR, including ERAP140 [23], RIP140 [24], CBP/P300 [25], BRG-1 [26], and the three members of the p160 family of coactivators: NCoA1 (SRC-1), NCoA2 (GRIP-1 and TIF-2) and NCoA3 (AIB-1, p/CIP, and ACTR) [27]. On the other hand, HIF-1α is known to interact with CBP/p300, SRC-1 and TIF2 [28] [29–32]. Thus, it is plausible that AhR and HIF-1α competes for a limited amount of CBP/p300, which may suppress transcriptional activities of these nuclear receptors. For further study, it is necessary to clarify the exact inhibitory mechanism of the AhR-mediated signaling pathway on the HIF-1α signaling pathway.

2. Vascular development in the placenta and related diseases

The placenta is an organ penetrated by maternal and fetal blood vessels, and acts as an interface between them by exchanging oxygen, nutrients and by-products. The vasculature of the placenta has been extensively studied because of its central role in pathogenesis for both maternal and fetal sides. Among mammalian species, the anatomical structures of rodents and humans are similar. The mature rodent placenta, so-called chorioallantoic placenta, is morphologically divided into two zones, the labyrinth zone and the junctional zone [33] (Fig. 1C). The junctional zone, which is devoid of fetal blood, contains three types of cells of fetal origin, i.e., the spongiotrophoblast cells, glycogen cells and trophoblast giant cells. Glycogen cells are considered to supply energy while spongiotrophoblast cells and trophoblast giant cells are known to secrete hormones, including diverse types of placental prolactin family proteins in a stage-specific manner [34]. The labyrinth zone is a place for exchanging oxygen and nutrients between maternal and fetal blood.

The most striking event during the development of the placental vasculature is the fusion of two membranes, chorion and allantois, and this event, termed as chorioallantoic fusion, begins around gestational day (GD) 10 and GD8.5 in rat and mouse, respectively [35] (Fig. 1C). After this fusion, fetal capillaries grow from the allantois, and the trophoblast cells that mostly originated from the chorion undergo extensive villous branching with its associated fetal capillaries to construct a vasculature in the labyrinth. Around the period of chorioallantoic fusion, the trophoblast giant cells invade into the maternal uterine wall, and maternal blood that leaks from ruptured uterine vessels flows into the narrow space of the labyrinthine maternal blood sinusoids that directly contact with the labyrinthine trophoblast cells. The labyrinthine vasculature is estimated to develop until around GD15 in the rat when DNA synthesis is terminated thereafter [36,37]. A crucial point raised here is that two different types of cell, endothelial and trophoblast cells, actively participate in the establishment of the complex vasculature of the placenta, whereas only endothelial cells play a major role in the development of the vasculature in other organs.

Even though vascular development in the placenta is more complicated than in other organs, knockout mouse studies showed that vascular development is strictly regulated by VEGF and HIFs in the placenta, which is similar to that in other organs. It was reported that embryos deficient in HIF-1α or ARNT are viable up to GD9.5 but could not survive beyond GD10.5, owing to severe placental defects including shallow placental invasion into the decidua and lack of vascularization of fetal vessels in the labyrinth zone because of a defect in the chorioallantoic fusion [38–41]. Furthermore, the number of spongiotrophoblast cells in the junctional zone was markedly reduced, whereas that of trophoblasts cells in the labyrinth zone was increased, suggesting that the balance of trophoblastic differentiation into each lineage was tilted [41]. These results strongly suggest that the differentiation of trophoblast cells is strictly regulated by HIF-1α/ARNT.

Impairment of placental blood circulation often results in disease conditions, such as intrauterine growth retardation of the fetus and preeclampsia, the latter of which is characterized by hypertension and proteinuria in pregnant women [42,43]. Approximately 5–7% of all pregnant women develop preeclampsia. Although the precise etiology is not known, preeclampsia is accompanied by vasospasm and endothelial injury as an end result [44]. Excessive secretion of Flt1 is considered to be responsible for endothelial injury [45]. Both disease conditions are presumably related to each other, and preeclampsia sometimes accompanies intrauterine growth restriction. In temporal aspects, these symptoms manifest during the late period of gestation, suggesting that vascular remodeling might participate in the development of this disease. Recent studies reported a possible link of preeclampsia of humans with that of rodents [35,46].

The etiologies of these diseases are complex owing to several factors including genetic as well as environmental issues [47]. As an environmental factor, cigarette smoking has been reported to impair placental vasculature and subsequent fetal growth restriction [48,49]. Microarray analysis, followed by quantitative RT-PCR analysis, of gene expression in the placentas of cigarette-smoking mothers revealed that AhR-dependent phase I enzyme genes, such as cytochrome P450 1A1 (CYP1A1) and CYP1B1, are activated, but that AhR- or Nrf2-dependent phase II genes are not. The imbalance between the

induced phase I enzymes and the noninduced phase II enzymes may result in increased oxidative stress, which could interfere with the function of the placenta and adversely affect the well-being of the fetus [50]. It is thus plausible to consider that AhR ligands act as environmental factors that affect the normal development of the placental vasculature.

3. Effects of TCDD on vascular remodeling in the placenta and the proposed mechanisms of toxicities

Because AhR ligands including dioxins and related compounds affect the early stage of organ development, it is intriguing to study how AhR-mediated signaling is involved in the development of blood vessels in the placenta. Administration of TCDD to pregnant C57BL/6 mice at a daily dose of 3 or 6 μg/kg bw from GDs 10 to 13 was found to induce histological alterations 24 h after the last administration when vasculogenesis is supposed to continue [51]. In the TCDD-exposed placenta, the vasculature that acts as a maternal-fetal barrier in the labyrinth was found to show hemorrhage of embryonic blood into the maternal circulation. This data suggests that the dose used was too high to consider subtle changes in terms of the expression of molecular markers of vasculogenesis and vascular remodeling. It has been reported that the exposure of Holtzman, Long–Evans, or Sprague–Dawley rats to TCDD before fertilization or at the early stage of gestation results in fetal death at the late, but not early, stage of gestation [7,52–54]. In these studies, no detailed analysis of the histology and molecular markers was available, and it is difficult to conclude whether and how TCDD affects chorioallantoic fusion, placental vasculogenesis, and vascular remodeling.

In the control placenta of Holtzman rats, the vascular remodeling were found to take place on GD15 even when the placental DNA synthesis was already terminated and, therefore, the vasculogenesis in the placenta presumably ceased [55]. On GD16, maternal sinusoids and fetal capillaries were narrow and the size and thickness of trophoblast cells were small, but these morphological features became reverse on GD20 with the development of the placenta (Fig. 2). In addition, the upregulation of genes involved in both the VEGF/VEGFR and Ang/Tie2 systems during this period was observed. On the other hand, administration of TCDD at 1600 ng/kg bw to Holtzman rats on GD15 to study its possible effects on the placental vasculature in the late period of gestation, the morphological features, such as maternal sinusoid, fetal capillaries and trophoblast cells, of the TCDD-exposed placenta on GD20, were very similar to the ones of the control placenta on GD16 (Fig. 2B) [55]. Lack of dilatation of both maternal blood sinusoids and fetal capillaries, existence of large size trophoblast cells, and the downregulated Tie2 mRNA level among the VEGF/VEGFR and Ang/Tie2 systems were

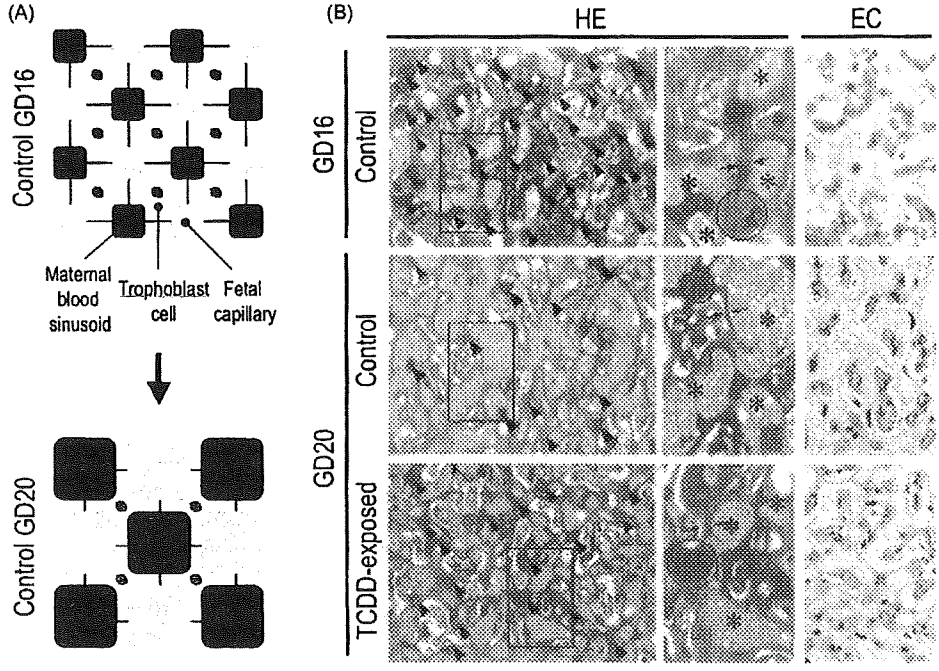

Fig. 2 – Vascular remodeling occurs in the placenta of Holtzman rats during the late period of gestation. (A) Schematic of horizontal dimension in the labyrinth zone of the placenta. Both the maternal blood sinusoids and fetal capillaries are enlarged from GDs 16 to 20 with a concomitant decrease in the number as well as thinning of trophoblast cells. (B) Suppresstion of vascular remodeling in the TCDD-exposed placenta. Horizontal sections of the placentas on GD16 and GD20 are shown. These sections were subjected to either hematoxylin and eosin (HE) staining, or endothelial cell (EC) staining using BS-1 lectin that identifies fetal capillaries. Note that the maternal blood sinusoids (asterisks) and fetal capillaries (in the EC stain) are not expanded in the TCDD-exposed placenta on GD20, which is similar to the morphology of control placenta on GD16. In addition, the number (arrow heads) and size (circle) of trophoblast cells are not decreased, and the trophoblastic interhemal membrane (between arrows) does not become thin in the TCDD-exposed placenta on GD20.

observed in TCDD-exposed placentas on GD20, suggesting that the vascular remodeling was suppressed by TCDD exposure. Furthermore, a striking effect of TCDD on apoptosis of trophoblast cells was present. Similar to the human placenta during the late period of gestation [56], a significant number of trophoblast cells (approximately 500/mm^2) were dead by apoptosis in the control placenta from GDs 16 to 20. In contrast, the number of apoptotic trophoblast cells in the TCDD-exposed placenta decreased to less than half of that in the control placenta [55]. In addition, TCDD-exposed placentas on GD20 were found to be in hypoxic condition [57], and to have an altered glucose metabolism on GD20 [58]. Under this condition, the presence of the altered glucose and glycogen metabolism was supported by the observations of decomposition products of glycogen cells in the junctional zone, increased glycogen content and upregulation of glucose transporter-2 (GLUT-2), GLUT-3, and GLUT-4 mRNAs levels [58,59].

The vascular remodeling to expand spaces for maternal blood sinusoids as well as fetal capillaries, observed in the control placentas during the late period of gestation, is considered to increase the net volume of circulating blood within the placenta. The observation is congruent with the increase in the physiological need for oxygen and nutrients of the significantly growing fetus. The apoptosis of tropohoblast cells is considered indispensable to offer spaces for the expansion of maternal blood sinusoids as well as fetal capillaries because the size of the placenta is restricted within the uterine horn and is relatively constant during the late period of gestation. Therefore, the inhibition of apoptosis by TCDD is considered to be essential for the pathogenesis of the TCDD-suppressive effect on vascular remodeling in the placenta of Holtzman rats.

The suppression of apoptosis in other types of cells following TCDD exposure has been reported in other studies. Vogel et al. [60] showed that the activation of AhR by TCDD resulted in the loss of the apoptosis response in lymphoma cell lines, which plays a key role in the development of lymphoma and leukemia, and clarified that the upregulation of cyclooxygenase-2 (COX-2), a downstream gene in the AhR signaling pathway, is associated with the suppression of apoptosis. Ray and Swanson [61] showed that TCDD exposure induces immortalization of human keratinocytes by suppressing apoptosis. Stinchcombe et al. [62] showed that the tumor promotion activated by TCDD in the rat liver is due to a decrease in apoptotic level. In this regard, the apoptotic activity of the human mammary epithelial cell line MCF10A was suppressed by TCDD exposure [63,64]. These several lines of evidence suggest that the suppression of apoptosis is considered to be a fundamental to TCDD toxicities.

How this inhibitory effect of TCDD on apoptosis is regulated? Paajarvi et al. [65] suggested that mouse double minute 2 (MDM2) which is up-regulated by AhR-mediated pathway is involved in this process. They showed that pretreatment of rats with TCDD diminished diethylnitrosamine-induced apoptosis in liver cells that is known to be p53-dependent, and that up-regulated MDM2 by AhR-mediated pathway decreased the apoptosis because MDM2 binds and degrades p53. It was reported that upregulation of MDM2 by nuclear receptor CAR is critical to suppress apoptosis in liver of mice that are exposed to pesticide contaminant 1,4-bis[2-(3,5-dichloropyridyloxy)]benzene (TCPOBOP) [66]. These results suggest that the MDM2 might play a central role in suppressing apoptosis after exposure to xenobiotics including TCDD. Further studies are necessary to assess whether MDM2 is upregulated in the placenta, especially in the trophoblast cells, after exposure to TCDD.

Chorioallantoic fusion and subsequent vasculogenesis have been proved to be regulated by the HIF-1α/ARNT signaling pathway [38–41]. The HIF-1α/ARNT pathway is possibly activated under hypoxic condition in the late period of gestation owing to an increased demand for oxygen during the fetal growth. This activation then stimulates the vascular remodeling, which results in an increase in the blood supply to overcome the hypoxic condition. In reality, these responses are highly tuned to be in a dynamic equilibrium. Our proteomics analysis data suggests that TCDD-induced placental tissues are under hypoxic status, and that the above-mentioned equilibrium is disrupted owing to the suppression of vascular remodeling in the placenta [55]. Trophoblast cells have a unique HIF-1α/ARNT signaling pathway compared with cells in other organs in order to thrive in the innate low-oxygen environment. This notion is supported by the experimental evidence showing that knockout mice of either ARNT or von Hippel-Lindau (VHL) gene, the product of which interacts with HIF-1α, has defect of blood vessel formation only in the placenta but not in yolk sac and embryos [67,68]. Further studies are required to clarify how the HIF-1α/ARNT signaling pathway regulates vascular remodeling in the placenta.

Type 1 diabetic mouse model that is induced by administration of streptozotocin exhibits intrauterine growth retardation [69]. Intriguingly, the placentas of these mice exhibit similar to those in TCDD-exposed rats including reduced blood flow [69], containing decomposition products of glycogen cells in the junctional zone [70,71], increased glycogen content [72,73], and increased GLUT3 mRNA level [74]. Moreover, fetuses in cadmium-exposed pregnant rats [75] and ethanol-fed pregnant mice [76] exhibit intrauterine growth retardation concomitant with the appearance of decomposition products of glycogen cells in the placenta. Therefore, it is conceivable that the placenta exhibits prototypical symptoms including abnormal vasculature and altered glucose kinetics regardless of the different types of insult as above. All of these insults, as well as smoking, could induce intrauterine growth retardation by disrupting the proper function of the placental vasculature in not only rodents but also humans [77]. A common process underlying the onset of these disease models is production of excessive amounts of reactive oxygen species that may cause damage to tissues, which has also been observed in TCDD-exposed placenta [76,77]. The suppression by TCDD of vascular remodeling in the placenta should be addressed on the basis of two important aspects, the involvement of the HIF-1a/ARNT pathway and the causal relationship between vascular impairment and oxidative stress.

4. Susceptibility of the fetus to TCDD toxicity and the AhR structure

Because the growing fetus requires large quantities of oxygen and nutrients particularly during the late period of gestation, a

failure in vascular remodeling is considered to increase the risk of fetal death. When Holtzman rats were administered TCDD at a dose of 0.8 and 1.6 μg/kg bw on GD15, they developed a disorder in the vasculature of the labyrinth zone, and the incidences of fetal death were 1% and 13%, respectively [58]. On the other hand, a low susceptibility of Sprague–Dawley rats to an *in utero* exposure to TCDD was found in an experiment, that is, even a six fold higher dose of TCDD at 10 μg/kg bw failed to cause any pathological alterations in the morphology of the placental vasculature and fetal death [78]. A logical explanation would be that the primary structures of the AhRs of these two rat strains differ from each other, as has been established in mouse and rat strains [9,79–81]. For example, in mouse strains, the affinity of the AhR of the C57BL/6J strain to TCDD is much higher than that of the AhR of other strains, such as DBA/2 [82]. In rat strains, Long-Evans rats have AhR that has a higher affinity to TCDD and are at least 1000-fold more sensitive (LD_{50} about 10 μg/kg) to the acute lethal effects of TCDD than Han/Wistar (kuopio; H/W) rats [83]. We thus formulated the above-mentioned hypothesis and examined the sequence of AhR. Contradictory to our hypothesis, the primary structure of AhR was found to be identical between Holtzman and Sprague–Dawley rats. We next examined the possible differences in the activity of AhR between these two rats strains by examining the TCDD-dependent expression of CYP1A1 mRNA, and confirmed that both rat strains induced CYP1A1 mRNA at an identical level in the placentas [78], suggesting that the strain difference in the TCDD toxicities on the placental vasculature and fetal death does not depend on the magnitude of AhR activities during gene transcription. Although we did not determine TCDD concentrations in the placenta, identical CYP1A1 mRNA levels suggest that TCDD was retained in this tissue presumably at a similar level.

To study the possible relationship of placental abnormalities with fetal death, we compared how the vascular structures of Sprague–Dawley and Holtzman rats develop as the gestation proceeds. In normal Sprague–Dawley rats, the vasculature in the labyrinth zone on GD16 is immature as shown by the narrow shape of both maternal blood sinusoids and fetal capillaries (unpublished data), and such morphology is very similar to that of Holtzman rats on GD16. However, the vasculature in the labyrinth zone of Sprague–Dawley rats did not change even on GD20. That is, the trophoblast cells are still large and their interhemal membrane is also thick in the labyrinth. In contrast, the vasculature in the labyrinth zone in normal Holtzman rats is altered from GDs 16 to 20, as described above. It seems likely that apoptotic elimination of trophoblast cells is decreased, or even does not occur in the placenta of Sprague–Dawley rats, suggesting that placental vascular development under the control of VEGF/VEGF-R and/or Ang/Tie2 systems of this strain might be different from that of Holtzman rats. The comparative analysis of the expression of molecular markers such as VEGF/VEGF-R and Ang/Tie2 systems during gestation could possibly unravel the mechanisms underlying vascular development and TCDD toxicity.

5. Conclusions

Vascular development, initiated by vasculogenesis angiogenesis (vascular remodeling), is regulated by an orchestration of VEGF/VEGF-R and Ang/Tie2 systems, respectively. In particular, the VEGF/VEGF-R system is upregulated by HIF-1α/ARNT under hypoxic condition in vasculogenesis, leading to the activation of the Ang/Tie2 system in vascular remodeling. It was demonstrated that *in utero* exposure to TCDD or cigarette smoke that contains AhR ligands affects vasculogenesis and vascular remodeling via AhR signaling by interacting with HIF-1α signaling depending on the vascular development stage. We found that *in utero* exposure to TCDD affects the process of vascular remodeling rather than vasculogenesis in the placenta of Holtzman rats. In this study, it was found that *in utero* exposure to TCDD markedly suppressed the development of sinusoids and trophoblast cells and the apoptosis of trophoblast cells under hypoxic condition, which results in a higher incidence of fetal death. However, no such effects were observed in Sprague–Dawley rats even if these two rat strains had identical AhR structure. The elucidation of the physiological process of vascular remodeling in these rat strains may shed light on how AhR signaling is involved in the TCDD toxicities in the placental vasculature.

Acknowledgements

This research was supported in part by the Special Coordination Fund for Promoting Science and Technology from the Ministry of Education, Culture, Sports, Science and Technology (to R.I.) and CREST, JST (to C.T.).

REFERENCES

[1] Hutzinger O, Choudhry GG, Chittim BG, Johnston LE. Formation of polychlorinated dibenzofurans and dioxins during combustion, electrical equipment fires and PCB incineration. Environ Health Perspect 1985;60:3–9.
[2] Theobald HM, Kimmel GL, Peterson RE. Developmental and reproductive toxicity of dioxins and related chemicals. In: Schecter A, Gasiewicz TA, editors. Dioxins and health. Hoboken, NJ, USA: Wiley-Interscience; 2003 . p. 329–432.
[3] Antkiewicz DS, Burns CG, Carney SA, Peterson RE, Heideman W. Heart malformation is an early response to TCDD in embryonic zebrafish. Toxicol Sci 2005;84:368–77.
[4] Antkiewicz DS, Peterson RE, Heideman W. Blocking expression of AHR2 and ARNT1 in zebrafish larvae protects against cardiac toxicity of 2,3,7,8-tetrachlorodibenzo-*p*-dioxin. Toxicol Sci 2006;94:175–82.
[5] Walker MK, Catron TF. Characterization of cardiotoxicity induced by 2,3,7,8-tetrachlorodibenzo-*p*-dioxin and related chemicals during early chick embryo development. Toxicol Appl Pharmacol 2000;167:210–21.
[6] Thackaberry EA, Nunez BA, Ivnitski-Steele ID, Friggins M, Walker MK. Effect of 2,3,7,8-tetrachlorodibenzo-*p*-dioxin on murine heart development: alteration in fetal and postnatal cardiac growth, and postnatal cardiac chronotropy. Toxicol Sci 2005;88:242–9.
[7] Olson JR, Holscher MA, Neal RA. Toxicity of 2,3,7,8-tetrachlorodibenzo-*p*-dioxin in the golden Syrian hamster. Toxicol Appl Pharmacol 1980;55:67–78.
[8] Guiney PD, Walker MK, Spitsbergen JM, Peterson RE. Hemodynamic dysfunction and cytochrome P4501A mRNA expression induced by 2,3,7,8-tetrachlorodibenzo-*p*-dioxin

during embryonic stages of lake trout development. Toxicol Appl Pharmacol 2000;168:1–14.
[9] Mimura J, Fujii-Kuriyama Y. Functional role of AhR in the expression of toxic effects by TCDD. Biochim Biophys Acta 2003;1619:263–8.
[10] Carmeliet P. Mechanisms of angiogenesis and arteriogenesis. Nat Med 2000;6:389–95.
[11] Semenza GL. Targeting HIF-1 for cancer therapy. Nat Rev Cancer 2003;3:721–32.
[12] Nie M, Blankenship AL, Giesy JP. Interactions between aryl hydrocarbon receptor (AhR) and hypoxia signaling pathways. Environ Toxicol Pharmacol 2001;10:17–27.
[13] Pollenz RS, Davarinos NA, Shearer TP. Analysis of aryl hydrocarbon receptor-mediated signaling during physiological hypoxia reveals lack of competition for the aryl hydrocarbon nuclear translocator transcription factor. Mol Pharmacol 1999;56:1127–37.
[14] Ichihara S, Yamada Y, Ichihara G, Nakajima T, Li P, Kondo T, et al. A role for the aryl hydrocarbon receptor in regulation of ischemia-induced angiogenesis. Arterioscler Thromb Vasc Biol 2007;27:1297–304.
[15] Fritz WA, Lin TM, Peterson RE. The aryl hydrocarbon receptor (AhR) inhibits vanadate-induced vascular endothelial growth factor (VEGF) production in TRAMP prostates. Carcinogenesis 2008;29:1077–82.
[16] Ivnitski-Steele ID, Walker MK. Vascular endothelial growth factor rescues 2,3,7,8-tetrachlorodibenzo-p-dioxin inhibition of coronary vasculogenesis. Birth Defects Res A Clin Mol Teratol 2003;67:496–503.
[17] Ivnitski-Steele ID, Sanchez A, Walker MK. 2,3,7,8-Tetrachlorodibenzo-p-dioxin reduces myocardial hypoxia and vascular endothelial growth factor expression during chick embryo development. Birth Defects Res A Clin Mol Teratol 2004;70:51–8.
[18] Ivnitski-Steele ID, Friggens M, Chavez M, Walker MK. 2,3,7,8-Tetrachlorodibenzo-p-dioxin (TCDD) inhibition of coronary vasculogenesis is mediated, in part, by reduced responsiveness to endogenous angiogenic stimuli, including vascular endothelial growth factor A (VEGF-A). Birth Defects Res A Clin Mol Teratol 2005;73:440–6.
[19] Juan SH, Lee JL, Ho PY, Lee YH, Lee WS. Antiproliferative and antiangiogenic effects of 3-methylcholanthrene, an aryl-hydrocarbon receptor agonist, in human umbilical vascular endothelial cells. Eur J Pharmacol 2006;530:1–8.
[20] Michaud SE, Menard C, Guy LG, Gennaro G, Rivard A. Inhibition of hypoxia-induced angiogenesis by cigarette smoke exposure: impairment of the HIF-1alpha/VEGF pathway. FASEB J 2003;17:1150–2.
[21] Ohtake F, Takeyama K, Matsumoto T, Kitagawa H, Yamamoto Y, Nohara K, et al. Modulation of oestrogen receptor signalling by association with the activated dioxin receptor. Nature 2003;423:545–50.
[22] Ohtake F, Baba A, Takada I, Okada M, Iwasaki K, Miki H, et al. Dioxin receptor is a ligand-dependent E3 ubiquitin ligase. Nature 2007;446:562–6.
[23] Nguyen TA, Hoivik D, Lee JE, Safe S. Interactions of nuclear receptor coactivator/corepressor proteins with the aryl hydrocarbon receptor complex. Arch Biochem Biophys 1999;367:250–7.
[24] Kumar MB, Tarpey RW, Perdew GH. Differential recruitment of coactivator RIP140 by Ah and estrogen receptors. Absence of a role for LXXLL motifs. J Biol Chem 1999;274:22155–64.
[25] Marlowe JL, Knudsen ES, Schwemberger S, Puga A. The aryl hydrocarbon receptor displaces p300 from E2F-dependent promoters and represses S phase-specific gene expression. J Biol Chem 2004;279:29013–22.
[26] Wang S, Hankinson O. Functional involvement of the Brahma/SWI2-related gene 1 protein in cytochrome P4501A1 transcription mediated by the aryl hydrocarbon receptor complex. J Biol Chem 2002;277:11821–7.
[27] Beischlag TV, Wang S, Rose DW, Torchia J, Reisz-Porszasz S, Muhammad K, et al. Recruitment of the NCoA/SRC-1/p160 family of transcriptional coactivators by the aryl hydrocarbon receptor/aryl hydrocarbon receptor nuclear translocator complex. Mol Cell Biol 2002;22:4319–33.
[28] Arany Z, Huang LE, Eckner R, Bhattacharya S, Jiang C, Goldberg MA, et al. An essential role for p300/CBP in the cellular response to hypoxia. Proc Natl Acad Sci USA 1996;93:12969–73.
[29] Ebert BL, Bunn HF. Regulation of transcription by hypoxia requires a multiprotein complex that includes hypoxia-inducible factor 1, an adjacent transcription factor, and p300/CREB binding protein. Mol Cell Biol 1998;18:4089–96.
[30] Kallio PJ, Okamoto K, O'Brien S, Carrero P, Makino Y, Tanaka H, et al. Signal transduction in hypoxic cells: inducible nuclear translocation and recruitment of the CBP/p300 coactivator by the hypoxia-inducible factor-1alpha. EMBO J 1998;17:6573–86.
[31] Ema M, Hirota K, Mimura J, Abe H, Yodoi J, Sogawa K, et al. Molecular mechanisms of transcription activation by HLF and HIF1alpha in response to hypoxia: their stabilization and redox signal-induced interaction with CBP/p300. EMBO J 1999;18:1905–14.
[32] Carrero P, Okamoto K, Coumailleau P, O'Brien S, Tanaka H, Poellinger L. Redox-regulated recruitment of the transcriptional coactivators CREB-binding protein and SRC-1 to hypoxia-inducible factor 1alpha. Mol Cell Biol 2000;20:402–15.
[33] Davies J, Glasser SR. Histological and fine structural observations on the placenta of the rat. Acta Anat (Basel) 1968;69:542–608.
[34] Soares MJ. The prolactin and growth hormone families: pregnancy-specific hormones/cytokines at the maternal–fetal interface. Reprod Biol Endocrinol 2004;2:51.
[35] Rossant J, Cross JC. Placental development: lessons from mouse mutants. Nat Rev Genet 2001;2:538–48.
[36] Butterstein GM, Leathem JH. Placental growth modification during pregnancy in the rat. Endocrinology 1974;95:645–9.
[37] Winick M, Noble A. Quantitative changes in ribonucleic acids and protein during normal growth of rat placenta. Nature 1966;212:34–5.
[38] Adelman DM, Gertsenstein M, Nagy A, Simon MC, Maltepe E. Placental cell fates are regulated in vivo by HIF-mediated hypoxia responses. Genes Dev 2000;14:3191–203.
[39] Kozak KR, Abbott B, Hankinson O. ARNT-deficient mice and placental differentiation. Dev Biol 1997;191:297–305.
[40] Maltepe E, Schmidt JV, Baunoch D, Bradfield CA, Simon MC. Abnormal angiogenesis and responses to glucose and oxygen deprivation in mice lacking the protein ARNT. Nature 1997;386:403–7.
[41] Cowden Dahl KD, Fryer BH, Mack FA, Compernolle V, Maltepe E, Adelman DM, et al. Hypoxia-inducible factors 1alpha and 2alpha regulate trophoblast differentiation. Mol Cell Biol 2005;25:10479–91.
[42] Redman CW, Sargent IL. Latest advances in understanding preeclampsia. Science 2005;308:1592–4.
[43] Kaufmann P, Black S, Huppertz B. Endovascular trophoblast invasion: implications for the pathogenesis of intrauterine growth retardation and preeclampsia. Biol Reprod 2003;69:1–7.
[44] Barbieri RL, Repeke JT. Medical disorders during pregnancy. In: Braunwald E, Fauchi A, Kasper D, Hauser S, Longo D, Jameson J, editors. Harrison's Principles Internal Medicine. 16th ed., McGraw-Hill; 2005. 32–37.
[45] Maynard SE, Min JY, Merchan J, Lim KH, Li J, Mondal S, et al. Excess placental soluble fms-like tyrosine kinase 1 (sFlt1) may contribute to endothelial dysfunction, hypertension,

and proteinuria in preeclampsia. J Clin Invest 2003;111:649–58.
[46] Cross JC. The genetics of pre-eclampsia: a feto-placental or maternal problem? Clin Genet 2003;64:96–103.
[47] Ilekis JV, Reddy UM, Roberts JM. Preeclampsia—a pressing problem: an executive summary of a National Institute of Child Health and Human Development workshop. Reprod Sci 2007;14:508–23.
[48] Salafia C, Shiverick K. Cigarette smoking and pregnancy II: vascular effects. Placenta 1999;20:273–9.
[49] Zdravkovic T, Genbacev O, McMaster MT, Fisher SJ. The adverse effects of maternal smoking on the human placenta: a review. Placenta 2005;26 Suppl. A:S81–6.
[50] Huuskonen P, Storvik M, Reinisalo M, Honkakoski P, Rysa J, Hakkola J, et al. Microarray analysis of the global alterations in the gene expression in the placentas from cigarette-smoking mothers. Clin Pharmacol Ther 2008;83:542–50.
[51] Khera KS. Extraembryonic tissue changes induced by 2,3,7,8-tetrachlorodibenzo-p-dioxin and 2,3,4,7,8-pentachlorodibenzofuran with a note on direction of maternal blood flow in the labyrinth of C57BL/6N mice. Teratology 1992;45:611–27.
[52] Sparschu GL, Dunn FL, Rowe VK. Study of the teratogenicity of 2,3,7,8-tetrachlorodibenzo-p-dioxin in the rat. Food Cosmet Toxicol 1971;9:405–12.
[53] Murray FJ, Smith FA, Nitschke KD, Humiston CG, Kociba RJ, Schwetz BA. Three-generation reproduction study of rats given 2,3,7,8-tetrachlorodibenzo-p-dioxin (TCDD) in the diet. Toxicol Appl Pharmacol 1979;50:241–52.
[54] Huuskonen H, Unkila M, Pohjanvirta R, Tuomisto J. Developmental toxicity of 2,3,7,8-tetrachlorodibenzo-p-dioxin (TCDD) in the most TCDD-resistant and -susceptible rat strains. Toxicol Appl Pharmacol 1994;124:174–80.
[55] Ishimura R, Kawakami T, Ohsako S, Nohara K, Tohyama C. Suppressive effect of 2,3,7,8-tetrachlorodibenzo-p-dioxin on vascular remodeling that takes place in the normal labyrinth zone of rat placenta during late gestation. Toxicol Sci 2006;91:265–74.
[56] Straszewski-Chavez SL, Abrahams VM, Mor G. The role of apoptosis in the regulation of trophoblast survival and differentiation during pregnancy. Endocr Rev 2005;26:877–97.
[57] Ishimura R, Ohsako S, Kawakami T, Sakaue M, Aoki Y, Tohyama C. Altered protein profile and possible hypoxia in the placenta of 2,3,7,8-tetrachlorodibenzo-p-dioxin-exposed rats. Toxicol Appl Pharmacol 2002;185:197–206.
[58] Ishimura R, Ohsako S, Miyabara Y, Sakaue M, Kawakami T, Aoki Y, et al. Increased glycogen content and glucose transporter 3 mRNA level in the placenta of Holtzman rats after exposure to 2,3,7,8-tetrachlorodibenzo-p-dioxin. Toxicol Appl Pharmacol 2002;178:161–71.
[59] Mizutani T, Yoshino M, Satake T, Nakagawa M, Ishimura R, Tohyama C, et al. Identification of 2,3,7,8-tetrachlorodibenzo-p-dioxin (TCDD)-inducible and -suppressive genes in the rat placenta: induction of interferon-regulated genes with possible inhibitory roles for angiogenesis in the placenta. Endocr J 2004;51:569–77.
[60] Vogel CF, Li W, Sciullo E, Newman J, Hammock B, Reader JR, et al. Pathogenesis of aryl hydrocarbon receptor-mediated development of lymphoma is associated with increased cyclooxygenase-2 expression. Am J Pathol 2007;171:1538–48.
[61] Ray SS, Swanson HI. Dioxin-induced immortalization of normal human keratinocytes and silencing of p53 and p16INK4a. J Biol Chem 2004;279:27187–93.
[62] Stinchcombe S, Buchmann A, Bock KW, Schwarz M. Inhibition of apoptosis during 2,3,7,8-tetrachlorodibenzo-p-dioxin-mediated tumour promotion in rat liver. Carcinogenesis 1995;16:1271–5.
[63] Park S, Matsumura F. Characterization of anti-apoptotic action of TCDD as a defensive cellular stress response reaction against the cell damaging action of ultra-violet irradiation in an immortalized normal human mammary epithelial cell line, MCF10A. Toxicology 2006;217:139–46.
[64] Davis Jr JW, Burdick AD, Lauer FT, Burchiel SW. The aryl hydrocarbon receptor antagonist, 3'methoxy-4'nitroflavone, attenuates 2,3,7,8-tetrachlorodibenzo-p-dioxin-dependent regulation of growth factor signaling and apoptosis in the MCF-10A cell line. Toxicol Appl Pharmacol 2003;188:42–9.
[65] Paajarvi G, Viluksela M, Pohjanvirta R, Stenius U, Hogberg J. TCDD activates Mdm2 and attenuates the p53 response to DNA damaging agents. Carcinogenesis 2005;26:201–8.
[66] Huang W, Zhang J, Washington M, Liu J, Parant JM, Lozano G, et al. Xenobiotic stress induces hepatomegaly and liver tumors via the nuclear receptor constitutive androstane receptor. Mol Endocrinol 2005;19:1646–53.
[67] Gnarra JR, Ward JM, Porter FD, Wagner JR, Devor DE, Grinberg A, et al. Defective placental vasculogenesis causes embryonic lethality in VHL-deficient mice. Proc Natl Acad Sci USA 1997;94:9102–7.
[68] Abbott BD, Buckalew AR. Placental defects in ARNT-knockout conceptus correlate with localized decreases in VEGF-R2, Ang-1, and Tie-2. Dev Dyn 2000;219:526–38.
[69] Chartrel NC, Clabaut MT, Boismare FA, Schrub JC. Uteroplacental hemodynamic disturbances in establishment of fetal growth retardation in streptozocin-induced diabetic rats. Diabetes 1990;39:743–6.
[70] Prager R, Abramovici A, Liban E, Laron Z. Histopathological changes in the placenta of streptozotocin induced diabetic rats. Diabetologia 1974;10:89–91.
[71] Gewolb IH, Merdian W, Warshaw JB, Enders AC. Fine structural abnormalities of the placenta in diabetic rats. Diabetes 1986;35:1254–61.
[72] Abramovici A, Sporn J, Prager R, Shaltiel A, Laron Z, Liban E. Glycogen metabolism in the placenta of streptozotocin diabetic rats. Horm Metab Res 1978;10:195–9.
[73] Gewolb IH, Barrett C, Warshaw JB. Placental growth and glycogen metabolism in streptozotocin diabetic rats. Pediatr Res 1983;17:587–91.
[74] Boileau P, Mrejen C, Girard J, Hauguel-de Mouzon S. Overexpression of GLUT3 placental glucose transporter in diabetic rats. J Clin Invest 1995;96:309–17.
[75] Hazelhoff Roelfzema W, Roelofsen AM, Peereboom-Stegeman JH. Glycogen content of placenta and of fetal and maternal liver in cadmium-exposed rats. I. A descriptive light microscopic study. Placenta 1987;8:27–36.
[76] Padmanabhan R. Histological and histochemical changes of the placenta in fetal alcohol syndrome due to maternal administration of acute doses of ethanol in the mouse. Drug Alcohol Depend 1985;16:229–39.
[77] Maulik D. Fetal growth restriction: the etiology. Clin Obstet Gynecol 2006;49:228–35.
[78] Kawakami T, Ishimura R, Nohara K, Takeda K, Tohyama C, Ohsako S. Differential susceptibilities of Holtzman and Sprague–Dawley rats to fetal death and placental dysfunction induced by 2,3,7,8-teterachlorodibenzo-p-dioxin (TCDD) despite the identical primary structure of the aryl hydrocarbon receptor. Toxicol Appl Pharmacol 2006;212:224–36.
[79] Moriguchi T, Motohashi H, Hosoya T, Nakajima O, Takahashi S, Ohsako S, et al. Distinct response to dioxin in an arylhydrocarbon receptor (AHR)-humanized mouse. Proc Natl Acad Sci USA 2003;100:5652–7.
[80] Tuomisto JT, Viluksela M, Pohjanvirta R, Tuomisto J. The AH receptor and a novel gene determine acute toxic responses to TCDD: segregation of the resistant alleles to different rat lines. Toxicol Appl Pharmacol 1999;155:71–81.

[81] Pohjanvirta R, Wong JM, Li W, Harper PA, Tuomisto J, Okey AB. Point mutation in intron sequence causes altered carboxyl-terminal structure in the aryl hydrocarbon receptor of the most 2,3,7,8-tetrachlorodibenzo-*p*-dioxin-resistant rat strain. Mol Pharmacol 1998;54:86–93.
[82] Poland A, Glover E, Kende AS. Stereospecific, high affinity binding of 2,3,7,8-tetrachlorodibenzo-*p*-dioxin by hepatic cytosol. Evidence that the binding species is receptor for induction of aryl hydrocarbon hydroxylase. J Biol Chem 1976;251:4936–46.
[83] Pohjanvirta R, Viluksela M, Tuomisto JT, Unkila M, Karasinska J, Franc MA, et al. Physicochemical differences in the AH receptors of the most TCDD-susceptible and the most TCDD-resistant rat strains. Toxicol Appl Pharmacol 1999;155:82–95.

JOURNAL OF APPLIED TOXICOLOGY
J. Appl. Toxicol. 2008
Published online in Wiley InterScience
(www.interscience.wiley.com) DOI: 10.1002/jat.1331

Differences in gene expression and benzo[a]pyrene-induced DNA adduct formation in the liver of three strains of female mice with identical *AhR*^{b2} genotype treated with 2,3,7,8-tetrachlorodibenzo-*p*-dioxin and/or benzo[a]pyrene

Qing Wu,[1] Junko S. Suzuki,[2] Hiroko Zaha,[2] Tien-Min Lin,[3] Richard E. Peterson,[3] Chiharu Tohyama[4] and Seiichiroh Ohsako[4,*]

[1] School of Public Health, Fudan University, 130 Dongan Road, Shanghai 200032, China
[2] Research Center for Environmental Risk, National Institute for Environmental Studies, 16-2 Onogawa, Tsukuba 305-8506, Japan
[3] School of Pharmacy and Molecular and Environmental Toxicology Center, University of Wisconsin, Madison, Wisconsin, USA
[4] Division of Environmental Health Sciences, Center for Disease Biology and Integrative Medicine, Graduate School of Medicine, The University of Tokyo, Hongo, Bunkyo-ku, Tokyo 113-0033, Japan

Received 19 June 2007; Revised 10 October 2007; Accepted 5 November 2007

ABSTRACT: To search for genes whose products modify aryl hydrocarbon receptor (AhR)-dependent toxicity caused by 2,3,7,8-tetrachlorodibenzo-p-dioxin (TCDD), gene expression profiles in the liver were surveyed using microarrays 24 h after the administration of TCDD to three strains of female mice, BALB/cAnN (BALB), C3H/HeN (C3H) and CBA/JN (CBA) all of identical AhR genotype. The BALB/cAnN strain had a more marked induction of a number of glutathione *S*-transferase (GST) sub-families, particularly the GSTmu gene family, compared with the other two strains. To assess the effects of GSTs induction to metabolize carcinogens, TCDD (40 μg kg^{-1}) was administered to BALB and CBA strains, followed 24 h later by an i.p. injection of low or high dose of benzo[a]pyrene (B[a]P, 50 or 200 mg kg^{-1}). The ^{32}P-postlabelling analysis showed that administration of TCDD alone failed to induce DNA adduct formation in both BALB and CBA strain mouse livers. The low dose of B[a]P alone produced DNA adduct in the liver of both strains to a similar extent. Treatment with TCDD 24 h before the low dose of B[a]P suppressed the formation of B[a]P-induced DNA-adduct more markedly in the BALB strain compared with the CBA strain. Taken together, these findings show that TCDD treatment causes strain-specific alterations in gene expression and B[a]P-induced DNA adduct formation in the liver of female mice of the same *AhR*^{b2} genotype. Furthermore, it suggests that TCDD-treated female mice of the BALB strain may have genes whose products modify the toxicity of B[a]P as evidenced by TCDD-induced alterations in B[a]P-DNA adduct formation. Copyright © 2008 John Wiley & Sons, Ltd.

Supplementary electronic material for this paper is available in Wiley Interscience at http://www.interscience.wiley.com/jpages/0260-437X/suppmat/jat.1331.html

KEY WORDS: aryl hydrocarbon receptor; benzo[a]pyrene; DNA-adduct; glutathione *S*-transferase; mouse, strain; 2,3,7,8-tetrachlorodibenzo-*p*-dioxin

Introduction

2,3,7,8-Tetrachlorodibenzo-*p*-dioxin (TCDD) is an environmental contaminant that is known to cause hepatotoxicity, teratogenicity and carcinogenicity (Schecter *et al.*, 2006). A characteristic feature in the toxicity of TCDD is exceptionally large differences in susceptibility among animal species or even strains belonging to the same species (Pohjanvirta and Tuomisto, 1994). Among inbred mouse strains, C57BL/6 is the most TCDD sensitive strain, while DBA/2 is less sensitive and requires a 10–20 times higher TCDD dose to manifest toxicity than the C57BL/6 strain (Chapman and Schiller, 1985). The C57BL/6 type of aryl hydrocarbon receptor (AhR) designated AhR^{b} has a 6-fold higher binding affinity than the DBA/2 type designated as AhR^{d} (Ema *et al.*, 1994). In addition, a C57BL/6 transgenic mouse strain in which the murine AhR was replaced with the human AhR showed less sensitivity to TCDD-induced teratogenicity than either the C57BL/6 or DBA/2 strains (Moriguchi *et al.*, 2003). A much greater difference (about 1000-fold) in susceptibility to the acute lethal effect of TCDD exists between two rat strains, Long-Evans (*Turku* AB; L-E) and Han/Wistar

* Correspondence to: Seiichiroh Ohsako, Division of Environmental Health Sciences, Center for Disease Biology and Integrative Medicine, Graduate School of Medicine, The University of Tokyo, Hongo, Bunkyo-ku, Tokyo 113-0033, Japan.
E-mail: ohsako@m.u-tokyo.ac.jp
Contract/grant sponsor: Environmental Technology Development Fund; Environmental Risk Office Fund of the Ministry of the Environment, Japan.

(*Kuopio*, H/W) (Unkila *et al.*, 1994). The H/W rat AhR has a *C*-terminal truncation of the transactivating domain compared with the L-E rat AhR (Pohjanvirta *et al.*, 1998). These interstrain differences in susceptibility to TCDD toxicity have been attributed to differences in AhR binding affinity and/or transcriptional activity in the various strains. Yet, a large difference in vulnerability to TCDD still exists that cannot be ascribed simply to polymorphisms of the *AhR* gene.

A quantitative trait locus analysis of an F2 intercross between C57BL/6 and DBA/2 strains showed that hepatic porphyria induced by pretreatment of iron compounds prior to TCDD administration depends on a gene locus that is independent from the *AhR* gene (Robinson *et al.*, 2002). In a Han/Wistar (*kupio*) strain that is very resistant to TCDD toxicity, a gene separate and distinct from the AhR may be responsible for the resistance to TCDD-induced lethality (Tuomisto *et al.*, 1999). Also TCDD treatment has been associated with placental disorders and fetal death in Holtzman rats, yet the same dose does not cause these effects in Sprague-Dawley rats even though both rat strains have an identical *AhR* genotype (Kawakami *et al.*, 2006). Furthermore, epididymal malformation by perinatal TCDD exposure was observed only in male Sprague-Dawley rats, not in Holtzman rats (Ohsako *et al.*, 2002). Together, these various findings suggest, in addition to the AhR, that other unknown gene products may exist that modulate TCDD toxicity in a strain- and species-dependent manner. Identification of these modifier genes is important for understanding the difference in susceptibility to TCDD toxicity among animal strains and species.

To test the hypothesis that there are genes whose products modify AhR dependent toxicities the study focused on benzo[a]pyrene (B[a]P)-induced DNA adduct formation in three mouse strains (BALB/c, CBA/J and C3H/He) that have an identical nucleotide sequence of the high affinity-type *AhR* gene, designated as AhR^{b2} (Thomas *et al.*, 2002). B[a]P is an extremely powerful carcinogen and its intermediate metabolite, benzo(a)pyrene 7,8-dihydrodiol-9,10-epioxide, is bioactivated by the classic TCDD inducible enzyme, cytochrome P4501A1 to form DNA adducts and act as an ultimate carcinogen (Sims *et al.*, 1974). The requirement of AhR to cause B[a]P induced skin carcinogenesis was demonstrated using AhR-null mice (Shimizu *et al.*, 2000). Unlike B[a]P, TCDD is not biotransformed to metabolites that directly react with DNA to form DNA adducts.

There were two overarching goals of the present study. The first was to determine the effect of TCDD treatment on gene expression in the liver of three strains of female mice having an identical *AhR* genotype (BALB, CBA and C3H). The second goal was to determine the effect of TCDD treatment on B[a]P-induced DNA-adduct formation in the liver of female mice from BALB and CBA that have the AhR^{b2} genotype in common.

Materials and Methods

Mice

Female BALB/cAnNCrj , CBA/JNCrj and C3H/HeNCrj strain mice were purchased from Charles River Japan, Inc. (Tokyo, Japan) and are referred to hereafter as BALB, C3H and CBA, respectively. The mice were provided food and water *ad libitum* and maintained in a controlled environment at a temperature of 24 ± 1 °C, a humidity of 45 ± 5% and a 12 h light/12 h dark cycle, and given free access to a solid diet (certified diet MF: Oriental Yeast Co., Tokyo, Japan) and distilled water. Animals were treated in a humane manner according to the National Institute for Environmental Studies' guidelines for animal experiments.

Exposure to TCDD and B[a]P

TCDD (>99.5% pure, 50 μg ml^{-1} in *n*-nonane) was purchased from Cambridge Isotope Laboratory (Andover, MA) and dissolved in corn oil (Sigma Aldrich, St Louis, MO) at serial concentrations of 0.1, 1.0 or 10.0 μg TCDD ml^{-1}. The *n*-nonane concentration was adjusted to 20% using *n*-nonane (Nacalai Tesque, Kyoto, Japan) and corn oil containing 20% *n*-nonane (Nacalai Tesque) was used as for the vehicle (control) treatment. B[a]P (Wako Pure Chemicals, Osaka, Japan) was dissolved in corn oil.

In an initial experiment, three 7-week-old, female mice were given a single oral dose of vehicle (control) or TCDD (40 μg kg^{-1}), euthanized by cervical dislocation 24 h later, and the livers removed. In a TCDD dose-response experiment, three females per dose were given a single oral dose of TCDD (0.4, 4.0 or 40 μg kg^{-1}) or an equivalent volume of vehicle (control). In both experiments, 24 h after exposure to vehicle or TCDD the mice were euthanized, the livers were quickly dissected from the carcasses and immediately placed into RNA*later* RNA Stabilization Reagent (Qiagen, Valencia, CA). For the TCDD-B[a]P exposure experiment, three females per group were given a single oral dose of TCDD (40 μg kg^{-1}), followed 24 h later by an intraperitoneal injection of B[a]P (50 or 200 mg kg^{-1}). Mice were killed by cervical dislocation 24 h after B[a]P administration, and livers were collected and kept at −80 °C for determination of DNA adducts.

Microarray Analysis

Total RNA was extracted from liver tissue samples from three female mice of each strain by using an RNeasy Mini Kit (Qiagen). Equivalent amounts of the RNA from each of the three livers per strain were mixed for the

DOI: 10.1002/jat

analysis for one array. cDNA synthesis, biotin-label cRNA synthesis and array analysis were performed according to the suppliers' protocols (Affymetrix, Santa Clara, CA). The Affymetrix GeneChip Mouse Expression Array 430A was used for the experiment. The GeneChip Operating Software (Affymetrix) was used to perform gene expression analysis. Gene expression levels in TCDD-exposed liver tissues from the three TCDD dose groups were compared with those of the vehicle control group, signal log two base ratios of >1 and <−1 were regarded as being significantly altered. Two independent experiments using a total of 18 arrays and 54 mice were performed for this array analysis. Pearson's correlation was used for hierarchical clustering with Gene Spring software (Agilent Technology, Tokyo, Japan).

Semiquantitative and Real-time RT-PCR

Semiquantitative and real-time RT-PCR were performed by our standard protocols (Kawakami *et al.*, 2006; Wu *et al.*, 2004) in order to amplify mouse CYP1A1, AhR, AhR nuclear translocator (ARNT), glutathione *S*-transferase mu 6 (GSTm6) and G3PDH mRNAs. Primer sequences used are summarized in Table 1. For semiquantitative RT-PCR, Hot Star Taq polymerase (Qiagen) was used. The reaction conditions were as follows: 1 cycle at 95 °C for 15 min, followed by 28 cycles of denaturation for 30 s at 94 °C, annealing for 30 s at 55 °C, and extension at 72 °C for 45 s. The PCR products were separated by electrophoresis on 2% agarose gels and photographed under a UV transilluminator. For the real-time RT-PCR, a QuantiTect SYBR Green PCR kit (Qiagen, Hilden, Germany) was used. The reaction conditions were as follows: 1 cycle at 95 °C for 15 min, followed by 35 cycles of denaturation for 15 s at 95 °C, annealing for 20 s at 56 °C, and extension at 72 °C for 20 s. After completion of the final cycle, a melting curve analysis was performed to monitor PCR product purity. Five serial dilutions ranging from 0.125 µl to 2 µl aliquots of the RT reaction products were used to construct a standard curve. The expression of the targeted gene transcript was calculated using linear extrapolation and normalized to that of the G3PDH gene. The expression ratios for the various genes were indicated relative to the mean expression ratio (adjusted to 1) in the control group.

Sequencing

The AhR-coding region (NM_013464) was amplified from liver cDNA using RT-PCR and LA Taq™ polymerase (TaKaRa Biomedicals, Otsu, Japan). The following four sets of primers were used for amplifying four DNA segments of the AhR coding region: forward-1, AGCCG GGAAG CCCTA GAGCA; reverse-1, AGACC AAGGC ATCTG CTGTG (621 bp amplicon); forward-2, AGTCC ACCCC TGCTG ACAGA AA; reverse-2, CGGAT GTGGG ATTCT GCACA (739 bp); forward-3, ACAAG AGGAT CGGGG TACCA; reverse-3, GATTT CGTCC GTTAT GTCGA (795 bp); forward-4, ACACT AGCAG GAAAG ACTGG; reverse-4, GAGCT CTCCC ATCGT ATAGG (1420 bp). Genomic DNA was isolated from mouse liver using a Wizard Genomic DNA purification kit (Promega, Madison, WI). The promoter region (−2237 to +340) of the GSTm6 gene (NT_039239.2) was amplified by PCR using the following primers: forward, GTGAC CCAGC TGTGA GAGAT; reverse, TGTCT CCCCT TCCAA CTCGT. The PCR products were directly sequenced using an Applied Biosystem 377-3100 Automated Sequencer, and the dideo-xynucleotide chain termination method was performed using a DYEnamic ET terminator cycle sequencing kit (Amersham Biosciences, Piscataway, NJ).

^{32}P-Postlabeling

B[a]P DNA adduct formation was determined by the ^{32}P-postlabeling method (Sato *et al.*, 2003; Uno *et al.*, 2004; Gupta *et al.*, 1982). In brief, DNA was extracted from liver samples by using a Wizard genome DNA isolation kit (Promega, Madison, WI). The DNA sample (8 µg) was digested with micrococcal endonuclease and spleen phosphodiesterase (Sigma-Aldrich) at 37 °C for 3 h, followed by a further digestion with nuclease P1 at 37 °C for 45 min. Tris-base was added to stop the reaction. The adduct nucleotides were labeled with [γ-^{32}P] ATP using T4 polynucleoside kinase at 37 °C for 30 min. Potato apyrase (Sigma-Aldrich) was added and the solution was cultured at 37 °C for 30 min to destroy excess ATP. After collecting a 1 µl aliquot of the ^{32}P-labeled solution for the determination of total nucleotides and ATP, the remaining ^{32}P labeled sample was applied to thin-layer

Table 1. Primers Used for RT-PCR

RT-PCR targets	Forward (5′ to 3′)	Reverse (5′ to 3′)	Product size	GenBank No.
CYP1A1	TGTTCACCCTACATAGAAACA	CAAGAGCTGATGCAGTAGTCTA	295bp	NM_009992
AhR	ATCCCACATCCGCATGATTAAG	GGGAGCCCAGTCTTTCCTGCTA	331bp	NM_013464
ARNT	CAGGCTACAGCCAAGACTCGTT	TGTGTCTGCTGAACATGCTGCT	284bp	NM_009709
GSTm6	TCGAATTCAGATGGGCATGCTT	GTACACAGGACTTGGAAGGAAGC	307bp	NM_008184
G3PDH	CACAGTCAAGGCCGAGAATG	TCTCGTGGTTCACACCCATC	382bp	M33599

DOI: 10.1002/jat

chromatography using a solvent system of 1 M sodium phosphate, pH 6.5 for developing direction 1; 3.5 M lithium formate, 8.5 M urea, pH 3.5 for direction 2; 0.8 M LiCl, 0.5 M Tris-HCl, 8.5 M urea, pH 8.0 for direction 3, 1.7 M sodium phosphate, pH 6.0 also for direction 3, on polyethylenimine (PEI) cellulose sheets (EM Science, Gibbstown, NJ). Autoradiography was used to detect DNA adducts, and their amounts were estimated as relative adduct level (RAL) = intensity of adduct nucleotides/(intensity of total nucleotides × dilution factor).

Statistical Analysis

StatView software for Windows version 5.0 (SAS Institute, Cary, NC) was used for statistical analyses. Means of gene expression levels and relative DNA-adduct levels for the TCDD and vehicle (control) treatment groups, respectively, were compared by one-way analysis of variance (ANOVA), followed by the Fisher PLSD test as a post-hoc test and Student's *t*-test. Significance was set at $P \leq 0.05$.

Results

TCDD-induced Alterations in Gene Expression in the Three Strains of Mice

According to the microarray analysis, the liver from TCDD-exposed, female BALB strain mice had 67 up-regulated and 71 down-regulated gene transcripts out of 22 690 gene transcripts, while fewer numbers of genes were altered in the liver of TCDD-exposed, female C3H and CBA strains of mice (See our website <http://www.nies.go.jp/health/drgdb/drgdb-top/TOP.htm> for DIOXIN RESPONSIVE GENE DATABASE, DRGdb-NIES). Direct sequence analyses demonstrated that the three mouse strains, BALB, C3H and CBA, had an identical nucleotide sequence in the entire open reading frame of *AhR* gene (results not shown), and a battery of AhR-dependent genes, such as CYP1A1, CYP1A2 and CYP1B1, were up-regulated by TCDD in all three strains. On the other hand, it was found that genes that were regulated by TCDD (40 μg kg^{-1}) in one strain were not necessarily regulated in the other two strains (Table 2). According

Table 2. Three strains of female mice (BALB, C3H and CBA) with identical *AhR*^{b2} genotype exhibit unique, strain-specific alterations in hepatic gene expression 24 h after exposure to a high dose of TCDD (40 μg kg^{-1})

UniGene ID	Gene title	Level[a]
BALB only		
Mm.10742	Cytochrome P450, family 4, subfamily a, polypeptide 10	2.10
Mm.31041	Glutathione *S*-transferase, mu 6	1.69
Mm.2935	RIKEN cDNA 4631408O11 gene	1.67
Mm.18064	Glucose-6-phosphatase, catalytic	1.60
Mm.4871	Tissue inhibitor of metalloproteinase 3	1.45
Mm.36742	ADAM-like, decysin 1	1.36
Mm.41116	Solute carrier family 25, member 30	1.36
Mm.6716	Histocompatibility 2, class II antigen A, beta 1	1.33
Mm.33653	Wingless-related MMTV integration site 2	1.23
Mm.23551	Ubiquitin-conjugating enzyme E2E 2 (UBC4/5 homolog, yeast)	1.16
Mm.2165	Serum amyloid P-component	−1.19
Mm.29094	Serine (or cysteine) proteinase inhibitor, clade A (alpha-1 antiproteinase, antitrypsin), member 10	−1.21
Mm.13787	Ceruloplasmin	−1.25
Mm.2774	Deiodinase, iodothyronine, type I	−1.54
Mm.200230	Adenosine A1 receptor	−1.91
Mm.69061	Guanine nucleotide binding protein, alpha transducing 1	−1.99
Mm.15675	Ephrin A1	−2.11
Mm.20286	Serine (or cysteine) proteinase inhibitor, clade A (alpha-1 antiproteinase, antitrypsin), member 12	−2.53
Mm.27334	Vanin 3	−2.98
Mm.31403	Tumor necrosis factor, alpha-induced protein 9	−3.34
C3H only		
Mm.29908	Dynein, cytoplasmic, light chain 1	1.26
Mm.30163	Ethanolamine kinase 1	1.09
Mm.6856	Pituitary tumor-transforming 1	−1.20
Mm.2131	Elastase 1, pancreatic	−1.26
Mm.28305	Hypothetical protein LOC223672	−1.32
Mm.41911	Cytochrome P450, family 46, subfamily a, polypeptide 1	−1.34
Mm.2580	Syndecan 1	−1.37
Mm.28685	Serine dehydratase	−1.42
Mm.22331	Monocyte to macrophage differentiation-associated 2	−1.86
CBA only		
Mm.25613	Immediate early response 3	2.21
Mm.195091	X-linked lymphocyte-regulated 3a	1.17
Mm.13020	Transcription factor 4	1.15
Mm.33353	Rho GTPase activating protein 6	−1.63

[a] Up- or down-regulation level was shown as the average Signal Log Ratio for comparisons (vehicle vs TCDD). Results were from two independent experiments.

DOI: 10.1002/jat

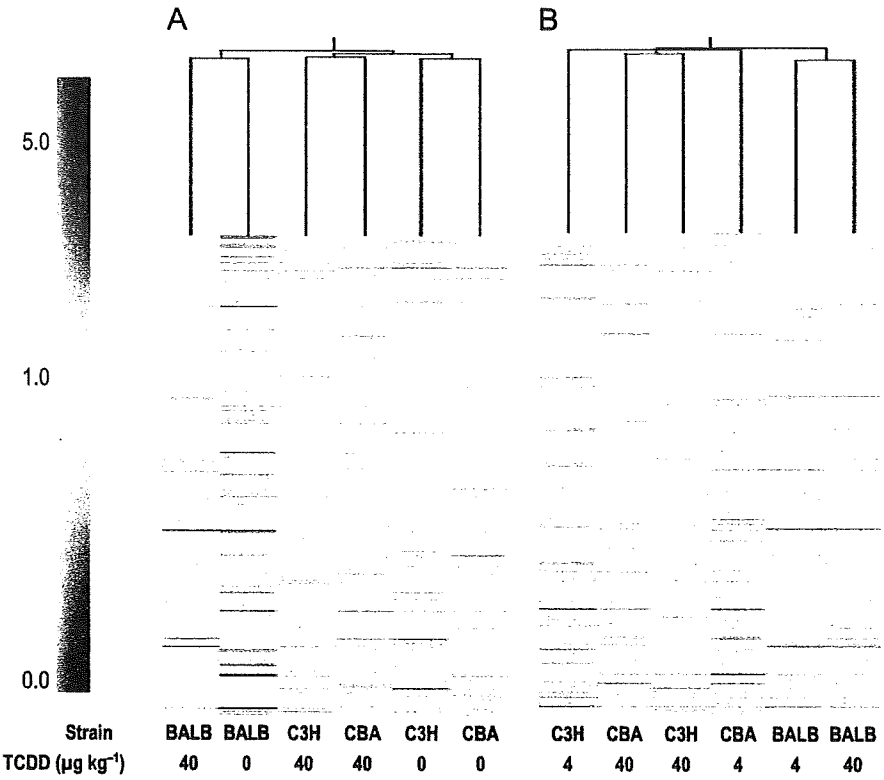

Figure 1. Hierarchical clustering analysis of microarray data. Hierarchical clustering analysis of the expression levels of the 22 690 probe sets contained on the microarrays for liver samples obtained from female BALB, C3H and CBA mice 24 h after treatment with either vehicle or 40 μg kg^{-1} TCDD. The signal intensity and the Trust were calculated and the clustering analyses were performed using GeneSpring software. The range of the signal intensity and the Trust, defined by the GeneSpring, are represented by colors, as shown by the color scale in the left bar. On the horizontal axis, the six samples were clustered based on a comparison of the overall pattern of gene expression in each sample. The length of the vertical lines connecting the different samples is proportional to the differences in liver expression patterns. (A) Comparison between vehicle and TCDD (40 μg kg^{-1}) treated liver samples. (B) Comparison between TCDD (4 μg kg^{-1}) and TCDD (40 μg kg^{-1}) treated liver samples. Note that the expression profiles of the C3H and CBA strains are similar, and BALB mice were in a different branch of the phylogenetic tree

to the gene clustering analysis, CBA and C3H strains presented similar expression-profile patterns, while BALB mice were allocated to a different branch of the phylogenetic tree (Fig. 1). These results suggest that global gene expression may be modulated differently by TCDD among strains with an identical AhR^{b2} genotype, due to different genetic backgrounds.

Induction of GST Gene Family by TCDD in BALB Mice

From the microarray data, the TCDD-exposed BALB strain had a higher expression level for five out of the six mu-class GST (GSTm) family genes than the TCDD-exposed C3H or CBA strains (Fig. 2). Other classes of GSTs, such as alpha-class GSTs (GSTa), theta-class GSTs (GSTt) and omega-class GSTs (GSTo), were also induced by TCDD at higher levels in BALB than in the other two mouse strains (Fig. 3). The GSTm6 mRNA expression levels were checked by real-time-RT-PCR and confirmed that they were dose-dependently increased by TCDD in the BALB strain, but not in the C3H and CBA strain mice (Fig. 4). There was no change in the expression levels of AhR and ARNT, while CYP1A1 mRNA was induced at a similar level in the livers of all three mouse strains (Fig. 4).

B[a]P-initiated DNA Adduct Formation upon TCDD Exposure

Since an elevated expression of GSTm was observed, possible differences were studied in susceptibility to the carcinogen B[a]P between the same three mouse strains that were pretreated with either vehicle (control) or TCDD. The level of B[a]P-induced DNA adduct formation in the liver of female mice of the BALB and CBA

DOI: 10.1002/jat

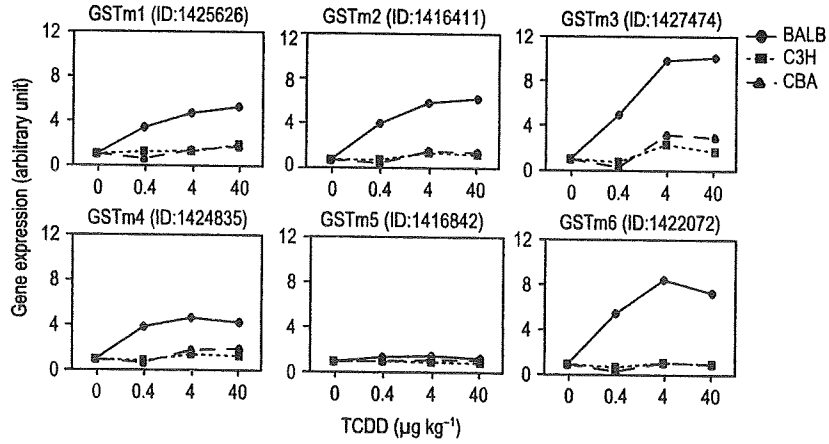

Figure 2. Induction of GSTm family genes in the liver of female BALB, C3H and CBA mice 24 h after exposure to vehicle or three graded doses of TCDD. Hepatic RNA specimens from three female mice were pooled as one array sample. The Affymetrix probe IDs of probe sets are shown in brackets to the right of the gene name. Horizontal and vertical axes represent TCDD dose (μg kg^{-1}) and fold-of-induction over vehicle-treated control, respectively. Note that five out of six GSTm genes, i.e. all except GSTm5, were up-regulated in the BALB strain

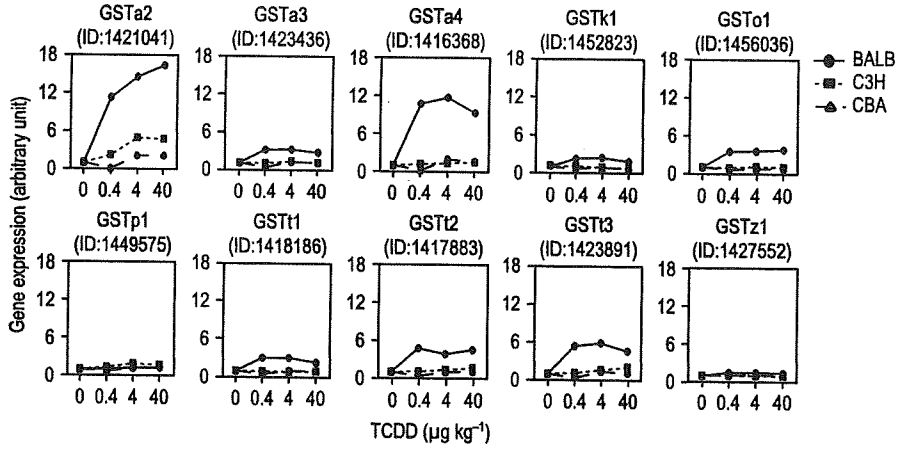

Figure 3. Induction of GST family genes, other than GSTm, in the liver of female mice of the BALB, C3H and CBA strains 24 h after exposure to vehicle (control, 0 μg kg^{-1}) or graded doses of TCDD (0.4, 4 or 40 μg kg^{-1}). Hepatic RNA specimens from three female mice of each strain were pooled as one array sample. The Affymetrix probe IDs of probe sets are shown in brackets to the right of each gene name. Horizontal and vertical axes represent TCDD dose (μg kg^{-1}) and fold-of-induction over the vehicle-treated control, respectively

strain was carried out using the ^{32}P-postlabeling method (Fig. 5). The B[a]P was administered 24 h after the treatment with vehicle (control) or TCDD.

Administration of TCDD alone failed to induce DNA adduct formation in both BALB and CBA strain mouse livers while B[a]P alone (50 mg kg^{-1}) produced DNA adduct in the liver of both strains to a similar extent (Fig. 5B). However, when B[a]P was administered 24 h after TCDD, the amount of DNA adducts formed were decreased to 20% and 36% of B[a]P treatment alone for both the BALB and CBA strains, respectively, and there was a significantly larger decrease for the BALB strain. On the other hand, when the B[a]P dose was increased to 200 mg kg^{-1} and given 24 h after TCDD, DNA adduct formation was increased approximately 2.3 and 2.0-fold over that observed in mice treated with the lower dose of B[a]P (50 mg kg^{-1}). This result was found for both BALB and CBA strains and there was no significant difference between the two strains (Fig. 5B).

Discussion

The susceptibility to xenochemicals is generally determined by various factors including absorption, distribution, metabolism and excretion. However, gene–environment interactions are an important research topic. It offers possible ways to define individual genetic risk profiles, which

DOI: 10.1002/jat

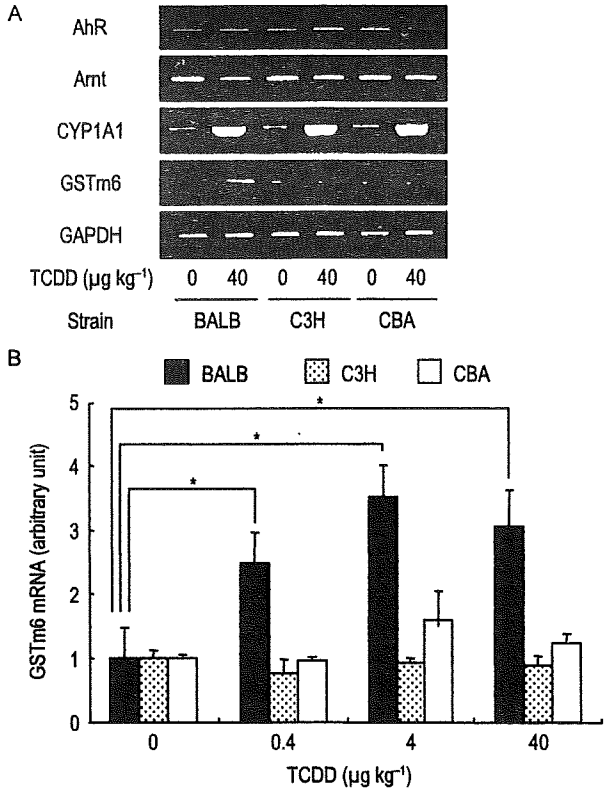

Figure 4. Gene expression levels of the CYP1A1, AhR, ARNT and GSTm6 in the liver of female mice from BALB, C3H and CBA strains having an identical AhR^{b2} genotype 24 h after exposure to vehicle (0 μg kg^{-1}) or TCDD (0.4, 4 or 40 μg kg^{-1}). (A) Image of electrophoretic gels of semi-quantitative RT-PCR. The hepatic mRNA levels for AhR, Arnt, and GAPDH was similar for vehicle and TCDD-exposed female mice of the BALB, C3H and CBA strains, respectively. CYP1A1 mRNA levels were induced by TCDD treatment in all three strains of female mice to a similar extent. On the other hand, the expression of GSTm6 mRNA in the liver of female mice was up-regulated only in the BALB strain. (B) Real-time PCR analysis of GSTm6 induction. Results are expressed as mean ± SE (n = 3). The expression level of GSTm6 was increased by TCDD in a dose-dependent manner only in the liver of female mice of the BALB strain. Asterisks in the bar graph showing GSTm6 mRNA abundance in the liver of female BALB strain mice indicate a statistically significant difference of the TCDD treatment groups (0.4, 4 and 40 μg kg^{-1}) from the vehicle-treated control (0 μg kg^{-1}) by ANOVA with a post-hoc analysis ($P < 0.05$)

may identify a sub-population of people at risk of developing certain diseases such as cancer, that may be associated with environmental exposure. Susceptibility to carcinogens such as TCDD and B[a]P might be influenced by ligand-binding affinity of the AhR. Activation of the AhR in the liver can result in the detoxification or activation of a parent xenobiotic by phase I enzymes such as cytochrome P450 1A1 and 2. A typical example of metabolic activation is the diol epoxide of B[a]P by CYP1A1 in human lung tissue, followed by the further detoxification by the phase II drug metabolizing process. In particular, the diol epoxide of B[a]P undergoes glutathione conjugation (Gelboin, 1980) and null mutation of GST-mu has been suspected to be linked to cancer risk. More specifically, 50% of Caucasians lack the GSTM1 gene, which is thought to be related an increased risk of lung cancer in smokers (Bartsch, 2000). Thus, gene and environment interactions such as these are important considerations in the health risk assessment of xenochemicals such as B[a]P.

To search for genes that might modulate AhR signaling, three strains of mice were used, BALB, C3H and CBA, that have in common an AhR^{b2} genotype, characterized by high AhR^{b2} binding affinity for TCDD. Cluster analysis revealed that the pattern of TCDD-induced alterations in hepatic gene expression in BALB mice was different from that of C3H and CBA mice, with unique sets of genes being regulated following high dose TCDD exposure (40 μg kg^{-1}) in each strain (Table 2). Accordingly the TCDD-induced hepatic gene expression profile of BALB mice was classified differentially from that of C3H and CBA mice. The unique gene expression changes in the liver of BALB versus C3H and CBA female mice may convey strain-specific effects of TCDD between these strains. However, the function of most of these genes are unknown. Therefore, the present study focused on glutathione-*S*-transferases (GSTs) to study possible modifying effects of the mouse strain on TCDD-induced phase II enzymes. GSTs comprise two distinct superfamilies, and the larger superfamily consists of cytosolic enzymes that are principally, but not exclusively, involved in biotransformation of toxic xenobiotics while the other family is composed of microsomal enzymes, primarily involved in arachidonic acid metabolism (Hayes and Pulford, 1995). The GSTmu-class belongs to the former superfamily. It has been reported that GSTmu (GSTm) and pi (GSTp) are efficient in the conjugation of intermediate metabolites of polycyclic aromatic hydrocarbons (PAHs), including B[a]P diol epoxide (Robertson *et al.*, 1986; Sundberg *et al.*, 1997). The present results showed that the induction of *GSTp1* gene was not markedly enhanced and was not different among the three mouse strains (Fig. 3). However, *GSTm* genes were more markedly induced by TCDD in the liver of female mice in the BALB strain than in the other two strains, C3H and CBA (Fig. 2), GSTm6 was up-regulated by TCDD (40 μg kg^{-1}) only in BALB strain but not in the other C3H and CBA strains (Table 2). Therefore, female BALB and CBA strain mice were administered, respectively, B[a]P 24 h after vehicle (control) or TCDD treatment to study the effect of TCDD on the induction of GSTm involved in the detoxification of B[a]P as well as on B[a]P induced DNA-adduct formation. Consistent

DOI: 10.1002/jat

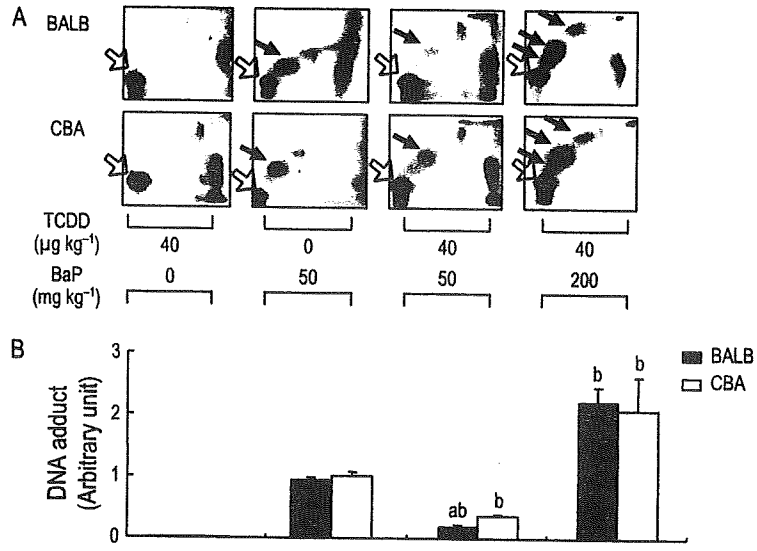

Figure 5. A representative result of DNA adduct formation. (A) Autoradiogram of B[a]P-DNA adducts detected by two-dimensional thin-layer chromatography using the ^{32}P-post labeling method. The open arrow indicates the point at which the ^{32}P-labeled DNA digested sample was applied. The solid arrow indicates the presence of B[a]P-DNA adducts. Liver samples from three mice were individually subjected to extraction of B[a]P-DNA adducts and applied to thin-layer chromatography. (B) Results are expressed as the mean ± SE (n = 3). Mean differences were analysed by Student's t-test. [a] BALB strain significantly different from the CBA strain for a specific TCDD and B[a]P treatment regimen ($P < 0.05$); [b] within the BALB strain or the CBA strain treated with both TCDD and B[a]P, respectively, the letter 'b' indicates a significant difference in DNA adduct formation ($P \leq 0.05$) compared with the TCDD only treatment group (40 μg kg^{-1} TCDD and 0 mg kg^{-1} B[a]P) and the B[a]P only treatment (0 μg kg^{-1} TCDD and 50 mg kg^{-1} B[a]P)

with GSTm-class genes being markedly induced by TCDD in BALB mice, it was found that the amount of B[a]P-DNA adduct formation was less in the liver of female mice of the BALB strain than of the CBA strain. B[a]P is a substrate for CYP1A1 and CYP1B1 and is metabolized by these phase I enzymes to form reactive intermediates that bind covalently to nucleic acids and proteins. B[a]P is detoxified by both phase I and phase II enzymes. B[a]P-DNA adduct formation depends on the balance between the activity of epoxidation and the activity of GST conjugation, which may be associated with CYP1A1 and CPY1B1 induction and GST family gene induction. In the present study, microarray data showed that CYP1A1 and CYP1B1 mRNA abundance were induced to similar levels in the liver of female BALB and CBA mice in two independent experiments. CYP1A1 induction was also checked by PCR. Therefore, the strain difference in formation of B[a]P-DNA adduct may be due to differential induction by TCDD of GST family genes. However, reduced formation of B[a]P-DNA adducts was only observed at the lowest dose of B[a]P tested (50 mg kg^{-1}) following TCDD exposure. At the higher B[a]P dose (200 mg kg^{-1}) following TCDD exposure there was not a significant strain difference in B[a]P-DNA adduct formation. The lack of a strain difference in response to TCDD treatment may have occurred because of the overwhelming high amount of B[a]P-induced DNA adduct formation in both mouse strains given the higher dose of B[a]P. The findings further suggest that the increased expression of GST family genes in the liver of female mice of the BALB strain may play a protecting role against AhR-dependent chemically induced carcinogenesis at low level in the liver of this strain.

Using liver samples from each of the BALB, CBA and C3H strains, genomic DNA of *GSTm6* was cloned, but no difference in sequence of the 5′-flanking sequence (-2255-bp) of *GSTm6* and no XRE motifs were found among the 5′-flanking sequence in the three strains (results not shown). It was also found that the XRE consensus sequence is not present in the 5′-flanking sequence of the promoter regions of the *GSTm1, GSTm2, GSTm3, GSTm4 and GSTm6* genes. While the mechanism of GSTm up-regulation by TCDD in BALB mice is unclear, it has been reported that phase I and phase II enzymes can be induced by TCDD and B[a]P through two distinct mechanisms: CYP1A1 is largely regulated by the XRE, whereas GST is largely regulated by the antioxidant response element (Prochaska and Talalay, 1988). The Keap1-Nrf2 system is known to regulate phase II drug-metabolizing enzymes by activating the antioxidant response element (Dinkova-Kostova *et al.*, 2002), and its activation by a chemoprotective agent, such as oltipraz, protects against B[a]P-induced stomach carcinogenesis (Ramos-Gomez *et al.*, 2001). Keap1-null mice have an increased level

DOI: 10.1002/jat

of GSTm gene expression, indicating that GSTm gene expression is regulated by the Keap1-Nrf2 system (Wakabayashi *et al.*, 2003). While the same system may play a role in enhancing GSTm expression only in BALB mice, the microarray results did not show a significant change of Nrf2 or Keap1 gene expression in the exposed group. Thus, possible involvement of the Nrf2/Keap1 system in the up-regulation of GSTm in TCDD-exposed female BALB mice, but not TCDD-exposed female C3H or CBA mice, will require further investigation. In the present study, administration of TCDD followed 24 h later by B[a]P (50 mg kg^{-1}) produced significantly fewer DNA adducts than after treatment with B[a]P alone. Although TCDD acts as a cancer promoter, Holcomb and Safe (1994) reported that TCDD inhibited 7,12-dimethylbenz[a]anthracene-induced tumorigenesis possibly by effects of TCDD exerted during the initial exposure period to 12-dimethylbenz[a]anthracene.

In summary, the present study shows that the liver of three strains of female mice that have the same AhR^{b2} genotype, respond differently to TCDD with respect to the number of genes that are up- and down-regulated 24 h after exposure. In particular the GSTm-class of genes were markedly induced by TCDD but only in BALB mice. These findings are of interest inasmuch as expression of GST family genes, in particular *GSTm*, reflect a distinct susceptibility to carcinogenicity by polycyclic aromatic hydrocarbons. The modulating biomolecules that transactivate *GSTm* genes and modify the carcinogenic susceptibility to PAHs may exist in BALB mice. The present experimental model using BALB and CBA strains having an identical AhR^{b2} genotype may be useful for ultimately identifying those genes that might be responsible for strain differences in susceptibility to chemical-induced toxicity and carcinogenicity.

Acknowledgements—The authors thank Dr Hiromi Sato, Institute of Medical Molecular Design, Inc., and Dr Shigeyuki Uno, Nihon University School of Medicine, for their technical suggestions regarding the detection of B[a]P-induced DNA adducts. This work was supported in part by grants from the Environmental Technology Development Fund (S.O.) and Environmental Risk Office Fund (C.T.) of the Ministry of the Environment, Japan.

References

Bartsch H. 2000. Studies on biomarkers in cancer etiology and prevention: a summary and challenge of 20 years of interdisciplinary research. *Mutat. Res.* **462**: 255–279.

Chapman DE, Schiller CM. 1985. Dose-related effects of 2,3,7,8-tetrachlorodibenzo-*p*-dioxin (TCDD) in C57BL/6J and DBA/2J mice. *Toxicol. Appl. Pharmacol.* **78**: 147–157.

Dinkova-Kostova AT, Holtzclaw WD, Cole RN, Itoh K, Wakabayashi N, Katoh Y, Yamamoto M, Talalay P. 2002. Direct evidence that sulfhydryl groups of Keap1 are the sensors regulating induction of phase 2 enzymes that protect against carcinogens and oxidants. *Proc. Natl Acad. Sci. USA* **99**: 11908–11913.

Ema M, Ohe N, Suzuki M, Mimura J, Sogawa K, Ikawa S, Fujii-Kuriyama Y. 1994. Dioxin binding activities of polymorphic forms of mouse and human arylhydrocarbon receptors. *J. Biol. Chem.* **269**: 27337–27343.

Gelboin HV. 1980. Benzo[alpha]pyrene metabolism, activation and carcinogenesis: role and regulation of mixed-function oxidases and related enzymes. *Physiol Rev.* **60**: 1107–1166.

Gupta RC, Reddy MV, Randerath K. 1982. 32P-postlabeling analysis of non-radioactive aromatic carcinogen — DNA adducts. *Carcinogenesis* **3**: 1081–1092.

Hayes JD, Pulford DJ. 1995. The glutathione S-transferase supergene family: regulation of GST and the contribution of the isoenzymes to cancer chemoprotection and drug resistance. *Crit. Rev. Biochem. Mol. Biol.* **30**: 445–600.

Holcomb M, Safe S. 1994. Inhibition of 7,12-dimethylbenzanthracene-induced rat mammary tumor growth by 2,3,7,8-tetrachlorodibenzo-*p*-dioxin. *Cancer Lett.* **82**: 43–47.

Kawakami T, Ishimura R, Nohara K, Takeda K, Tohyama C, Ohsako S. 2006. Differential susceptibilities of Holtzman and Sprague-Dawley rats to fetal death and placental dysfunction induced by 2,3,7,8-tetrachlorodibenzo-*p*-dioxin (TCDD) despite the identical primary structure of the aryl hydrocarbon receptor. *Toxicol. Appl. Pharmacol.* **212**: 224–236.

Moriguchi T, Motohashi H, Hosoya T, Nakajima O, Takahashi S, Ohsako S, Aoki Y, Nishimura N, Tohyama C, Fujii-Kuriyama Y, Yamamoto M. 2003. Distinct response to dioxin in an arylhydrocarbon receptor (AHR)-humanized mouse. *Proc. Natl Acad. Sci. USA* **100**: 5652–5657.

Ohsako S, Miyabara Y, Sakaue M, Ishimura R, Kakeyama M, Izumi H, Yonemoto J, Tohyama C. 2002. Developmental stage-specific effects of perinatal 2,3,7,8-tetrachlorodibenzo-*p*-dioxin exposure on reproductive organs of male rat offspring. *Toxicol. Sci.* **66**: 283–292.

Pohjanvirta R, Tuomisto J. 1994. Short-term toxicity of 2,3,7,8-tetrachlorodibenzo-*p*-dioxin in laboratory animals: effects, mechanisms, and animal models. *Pharmacol. Rev.* **46**: 483–549.

Pohjanvirta R, Wong JM, Li W, Harper PA, Tuomisto J, Okey AB. 1998. Point mutation in intron sequence causes altered carboxyl-terminal structure in the aryl hydrocarbon receptor of the most 2,3,7,8-tetrachlorodibenzo-*p*-dioxin-resistant rat strain. *Mol. Pharmacol.* **54**: 86–93.

Prochaska HJ, Talalay P. 1988. Regulatory mechanisms of monofunctional and bifunctional anticarcinogenic enzyme inducers in murine liver. *Cancer Res.* **48**: 4776–4782.

Ramos-Gomez M, Kwak MK, Dolan PM, Itoh K, Yamamoto M, Talalay P, Kensler TW. 2001. Sensitivity to carcinogenesis is increased and chemoprotective efficacy of enzyme inducers is lost in nrf2 transcription factor-deficient mice. *Proc. Natl Acad. Sci. USA* **98**: 3410–3415.

Robertson IG, Guthenberg C, Mannervik B, Jernstrom B. 1986. Differences in stereoselectivity and catalytic efficiency of three human glutathione transferases in the conjugation of glutathione with 7 beta,8 alpha-dihydroxy-9 alpha,10 alpha-oxy-7,8,9,10-tetrahydrobenzo(a)pyrene. *Cancer Res.* **46**: 2220–2224.

Robinson SW, Clothier B, Akhtar RA, Yang AL, Latour I, Van Ijperen C, Festing MF, Smith AG. 2002. Non-ahr gene susceptibility loci for porphyria and liver injury induced by the interaction of 'dioxin' with iron overload in mice. *Mol. Pharmacol.* **61**: 674–681.

Sato H, Suzuki KT, Sone H, Yamano Y, Kagawa J, Aoki Y. 2003. DNA-adduct formation in lungs, nasal mucosa, and livers of rats exposed to urban roadside air in Kawasaki City, Japan. *Environ. Res.* **93**: 36–44.

Schecter A, Birnbaum L, Ryan JJ, Constable JD. 2006. Dioxins: an overview. *Environ. Res.* **101**: 419–428.

Shimizu Y, Nakatsuru Y, Ichinose M, Takahashi Y, Kume H, Mimura J, Fujii-Kuriyama Y, Ishikawa T. 2000. Benzo[a]pyrene carcinogenicity is lost in mice lacking the aryl hydrocarbon receptor. *Proc. Natl Acad. Sci. USA* **97**: 779–782.

Sims P, Grover PL, Swaisland A, Pal K, Hewer A. 1974. Metabolic activation of benzo(a)pyrene proceeds by a diol-epoxide. *Nature* **252**: 326–328.

Sundberg K, Widersten M, Seidel A, Mannervik B, Jernstrom B. 1997. Glutathione conjugation of bay- and fjord-region diol epoxides of polycyclic aromatic hydrocarbons by glutathione transferases M1-1 and P1-1. *Chem. Res. Toxicol.* **10**: 1221–1227.

Thomas RS, Penn SG, Holden K, Bradfield CA, Rank DR. 2002. Sequence variation and phylogenetic history of the mouse Ahr gene. *Pharmacogenetics* **12**: 151–163.

Tuomisto JT, Viluksela M, Pohjanvirta R, Tuomisto J. 1999. The AH receptor and a novel gene determine acute toxic responses to TCDD:

segregation of the resistant alleles to different rat lines. *Toxicol. Appl. Pharmacol.* **155**: 71–81.

Unkila M, Pohjanvirta R, MacDonald E, Tuomisto JT, Tuomisto J. 1994. Dose response and time course of alterations in tryptophan metabolism by 2,3,7,8-tetrachlorodibenzo-*p*-dioxin (TCDD) in the most TCDD-susceptible and the most TCDD-resistant rat strain: relationship with TCDD lethality. *Toxicol. Appl. Pharmacol.* **128**: 280–292.

Uno S, Dalton TP, Derkenne S, Curran CP, Miller ML, Shertzer HG, Nebert DW. 2004. Oral exposure to benzo[a]pyrene in the mouse: detoxication by inducible cytochrome P450 is more important than metabolic activation. *Mol. Pharmacol.* **65**: 1225–1237.

Wakabayashi N, Itoh K, Wakabayashi J, Motohashi H, Noda S, Takahashi S, Imakado S, Kotsuji T, Otsuka F, Roop DR, Harada T, Engel JD, Yamamoto M. 2003. Keap1-null mutation leads to postnatal lethality due to constitutive Nrf2 activation. *Nat. Genet.* **35**: 238–245.

Wu Q, Ohsako S, Ishimura R, Suzuki JS, Tohyama C. 2004. Exposure of mouse preimplantation embryos to 2,3,7,8-tetrachlorodibenzo-*p*-dioxin (TCDD) alters the methylation status of imprinted genes H19 and Igf2. *Biol. Reprod.* **70**: 1790–1797.

DOI: 10.1002/jat

Development 135, 3511-3519 (2008) doi:10.1242/dev.027144

Functional importance of evolutionally conserved Tbx6 binding sites in the presomitic mesoderm-specific enhancer of *Mesp2*

Yukuto Yasuhiko[1,*], Satoshi Kitajima[1], Yu Takahashi[1], Masayuki Oginuma[2], Harumi Kagiwada[3], Jun Kanno[1] and Yumiko Saga[2,*]

The T-box transcription factor Tbx6 controls the expression of *Mesp2*, which encodes a basic helix-loop-helix transcription factor that has crucial roles in somitogenesis. In cultured cells, Tbx6 binding to the *Mesp2* enhancer region is essential for the activation of *Mesp2* by Notch signaling. However, it is not known whether this binding is required in vivo. Here we report that an *Mesp2* enhancer knockout mouse bearing mutations in two crucial Tbx6 binding sites does not express *Mesp2* in the presomitic mesoderm. This absence leads to impaired skeletal segmentation identical to that reported for *Mesp2*-null mice, indicating that these Tbx6 binding sites are indispensable for *Mesp2* expression. T-box binding to the consensus sequences in the *Mesp2* upstream region was confirmed by chromatin immunoprecipitation assays. Further enhancer analyses indicated that the number and spatial organization of the T-box binding sites are critical for initiating *Mesp2* transcription via Notch signaling. We also generated a knock-in mouse in which the endogenous *Mesp2* enhancer was replaced by the core enhancer of medaka *mespb*, an ortholog of mouse *Mesp2*. The homozygous enhancer knock-in mouse was viable and showed normal skeletal segmentation, indicating that the medaka *mespb* enhancer functionally replaced the mouse *Mesp2* enhancer. These results demonstrate that there is significant evolutionary conservation of Mesp regulatory mechanisms between fish and mice.

KEY WORDS: T-box transcription factor, Enhancer, Targeted disruption, Somitogenesis

INTRODUCTION

Somitogenesis is an important morphogenic process that generates metameric structures in vertebrates, including vertebra, muscles and motoneurons. The segmental boundary of each somite forms at the anterior end of the presomitic mesoderm (PSM) or unsegmented paraxial mesoderm, which are supplied from the primitive streak or tailbud at a later stage of development (Saga and Takeda, 2001). This process proceeds through the interaction of a number of signaling cascades, including Notch, Wnt and Fgf (Delfini et al., 2005; Dunty et al., 2008; Galceran et al., 2004; Hofmann et al., 2004; Moreno and Kintner, 2004; Takahashi et al., 2000). Thus, somitogenesis could be a very useful model system in which to study the interactions among the various signaling cascades that facilitate periodic pattern formation.

The basic helix-loop-helix transcription factor Mesp2 plays a crucial role in both somite segment border formation and in the establishment of the rostrocaudal patterning of each somite (Saga et al., 1997). *Mesp2* shows dynamic and periodic expression in the anterior PSM. This expression pattern defines the positioning of the newly forming somite by suppressing Notch signaling, in part through the activation of lunatic fringe (*Lfng*) (Morimoto et al., 2005). Genetic analyses have revealed that *Mesp2* expression is itself controlled by Notch signaling, indicating the existence of complicated feedback circuitry (Takahashi et al., 2003; Takahashi et al., 2000). We have previously identified the minimal PSM-specific *Mesp2* enhancer (denoted P2PSME) that is sufficient to reproduce the normal *Mesp2* expression pattern in transgenic animals (Haraguchi et al., 2001). We have also demonstrated that the T-box transcriptional regulator Tbx6 directly binds to P2PSME and is essential for P2PSME activity (Yasuhiko et al., 2006). We also showed that Notch signaling strongly enhanced *Mesp2* activation via Tbx6 and we identified the sequences that are important for this enhancement using an in vitro reporter assay (Yasuhiko et al., 2006). However, the question of whether P2PSME is indispensable for *Mesp2* expression during somitogenesis remained to be addressed. Because of differences in the expression patterns of *Mesp2* and Tbx6 – Tbx6 is expressed throughout the PSM and tailbud (Chapman et al., 1996; White and Chapman, 2005) whereas *Mesp2* expression is observed only in the anterior PSM (Saga et al., 1997) – another open question was whether Tbx6 actually binds to P2PSME.

The evolutionary aspect of this system is also noteworthy. We previously identified the *mespb* PSM-specific enhancer in the teleost fish medaka, and reported that the mutation of two T-box binding sites therein diminished its PSM-specific enhancer activity in transgenic embryos (Terasaki et al., 2006). However, definitive evidence as to whether the T-box-factor-dependent regulation is a conserved mechanism among vertebrates remains elusive.

In this study, we established *Mesp2* enhancer knockout mice and confirmed that Tbx6 binding sequences are essential for *Mesp2* expression. The in vivo association of Tbx6 with P2PSME was confirmed in chromatin immunoprecipitation assays, and reporter assays further showed that the number and spatial organization of Tbx6 binding sites are important for P2PSME activity. Furthermore, using a knock-in mouse that harbors the medaka *mespb* enhancer in place of the mouse *Mesp2* enhancer, we show that the T-box-factor-dependent regulation of the Mesp gene is evolutionally conserved between fish and mice.

[1]Division of Cellular and Molecular Toxicology, National Institute of Health Sciences, 1-18-1 Kamiyoga, Setagaya-ku, Tokyo 158-8501, Japan. [2]Division of Mammalian Development, National Institute of Genetics, 1111 Yata, Mishima, Shizuoka 411-8540, Japan. [3]Research Institute for Cell Engineering, National Institute of Advanced Industrial Science and Technology, 3-11-46 Nakoji, Amagasaki, Hyogo 661-0974 Japan.

*Authors for correspondence (e-mails: yasuhiko@nihs.go.jp; ysaga@lab.nig.ac.jp)

Accepted 8 September 2008